Basin Research

IAS EAGE

Basin Research (2017) **29**, 674–698, doi: 10.1111/bre.12219

Impact of normal faulting and pre-rift salt tectonics on the structural style of salt-influenced rifts: the Late Jurassic Norwegian Central Graben, North Sea

Zhiyuan Ge,* Rob L. Gawthorpe,* Atle Rotevatn* and Michel Bøgh Thomas†

**Department of Earth Science, University of Bergen, Bergen, Norway*
†*Total E&P Norge AS, Stavanger, Norway*

ABSTRACT

Studies of salt-influenced rift basins have focused on individual or basin-scale fault system and/or salt-related structure. In contrast, the large-scale rift structure, namely rift segments and rift accommodation zones and the role of pre-rift tectonics in controlling structural style and syn-rift basin evolution have received less attention. The Norwegian Central Graben, comprises a complex network of sub-salt normal faults and pre-rift salt-related structures that together influenced the structural style and evolution of the Late Jurassic rift. Beneath the halite-rich, Permian Zechstein Supergroup, the rift can be divided into two major rift segments, each comprising rift margin and rift axis domains, separated by a rift-wide accommodation zone – the Steinbit Accommodation Zone. Sub-salt normal faults in the rift segments are generally larger, in terms of fault throw, length and spacing, than those in the accommodation zone. The pre-rift structure varies laterally from sheet-like units, with limited salt tectonics, through domains characterised by isolated salt diapirs, to a network of elongate salt walls with intervening minibasins. Analysis of the interactions between the sub-salt normal fault network and the pre-rift salt-related structures reveals six types of syn-rift depocentres. Increasing the throw and spacing of sub-salt normal faults from rift segment to rift accommodation zone generally leads to simpler half-graben geometries and an increase in the size and thickness of syn-rift depocentres. In contrast, more complex pre-rift salt tectonics increases the mechanical heterogeneity of the pre-rift, leading to increased complexity of structural style. Along the rift margin, syn-rift depocentres occur as interpods above salt walls and are generally unrelated to the relatively minor sub-salt normal faults in this structural domain. Along the rift axis, deformation associated with large sub-salt normal faults created coupled and decoupled supra-salt faults. Tilting of the hanging wall associated with growth of the large normal faults along the rift axis also promoted a thin-skinned, gravity-driven deformation leading to a range of extensional and compressional structures affecting the syn-rift interval. The Steinbit Accommodation Zone contains rift-related structural styles that encompass elements seen along both the rift margin and axis. The wide variability in structural style and evolution of syn-rift depocentres recognised in this study has implications for the geomorphological evolution of rifts, sediment routing systems and stratigraphic evolution in rifts that contain pre-rift salt units.

INTRODUCTION

During rifting, extension in the brittle upper crust is accommodated initially by many small, kilometre-long, isolated faults distributed over a wide area, before deformation becomes localised on relatively few linked faults that are tens of kilometres long and bound to crustal-scale tilted fault blocks or half grabens (e.g. Gupta *et al.*, 1998; Cowie *et al.*, 2000; Gawthorpe & Leeder, 2000). In many rift basins, such as the North Sea, evaporite rocks, including halite and gypsum, form part of the pre-rift stratigraphy and can influence the structural and stratigraphic evolution of the rift (e.g. Hodgson *et al.*, 1992; Stewart *et al.*, 1999; Alves *et al.*, 2002; Hudec & Jackson, 2007; Marsh *et al.*, 2010; Duffy *et al.*, 2013; Lewis *et al.*, 2013). The evaporite units may fully or partially decouple the sub-salt deformation from that in supra-salt strata, giving rise to markedly different structural styles above and below the evaporite unit (Koyi *et al.*, 1993; Stewart *et al.*, 1996, 1997; Withjack & Callaway, 2000; Richardson *et al.*, 2005; Duffy *et al.*, 2013). Salt also provides a ductile detachment layer allowing thin-skinned deformation to develop in the supra-salt strata when tilting

Correspondence: Zhiyuan Ge, Department of Earth Science, University of Bergen, Allégaten 41, 5007 Bergen, Norway. E-mail: Zhiyuan.Ge@uib.no.

induces gravitational sliding (e.g. Stewart & Coward, 1995; Stewart & Clark, 1999; Stewart, 2007).

Previous studies have highlighted how sub-salt normal fault networks control deformation within the post-salt strata by stimulating salt mobilisation and initiating folding and faulting (e.g. Withjack *et al.*, 1990; Koyi *et al.*, 1993; Dooley *et al.*, 2003; Kane *et al.*, 2010; Duffy *et al.*, 2013; Lewis *et al.*, 2013; Tvedt *et al.*, 2013). Most of these studies have focused on fault displacement and salt thickness as controls on the degree of coupling between individual sub- and supra-salt normal faults (e.g. Stewart *et al.*, 1996, 1997; Stewart & Clark, 1999; Richardson *et al.*, 2005; Lewis *et al.*, 2013). However, largely overlooked in the discussion of salt-influenced rifts is the influence of the large-scale rift structure, namely rift segments and rift accommodation zones, and the pre-rift salt tectonics on structural style and basin evolution.

In many salt-influenced rifts, salt-related structures, such as salt diapirs and salt walls, are present before the onset of rifting (e.g. the Central Graben, the Lusitanian Basin and the North German Basin; Hodgson *et al.*, 1992; Rasmussen *et al.*, 1998; Alves *et al.*, 2002; Mohr *et al.*, 2005). Pre-existing salt diapirs and salt walls in contractional settings have been shown to localise strain during compression and are associated with the development of folds and thrusts (e.g. Letouzey *et al.*, 1995; Rowan & Vendeville, 2006; Callot *et al.*, 2012). In rifts, however, very few studies have addressed the role of pre-existing salt-related structures in controlling the structural style and tectono-stratigraphic evolution during rifting.

In this study, we focus on the Late Jurassic Norwegian Central Graben (Fig. 1). The study area has regional high-quality, borehole-calibrated, three-dimensional (3D) seismic data allowing structural styles and tectono-stratigraphy to be analysed (Fig. 1a). Salt-related structures existed prior to the Late Jurassic rift phase (Hodgson *et al.*, 1992; Smith *et al.*, 1993), allowing the investigation of how sub-salt normal faulting and pre-rift salt-related structures interact to influence the syn-rift structural style and tectono-stratigraphic evolution.

GEOLOGICAL SETTING

The Norwegian Central Graben is part of the NNW–SSE-trending Central Graben, which consists of a series of *en-echelon* extensional sub-basins in the southern arm of the Late Jurassic North Sea rift system (Fig. 1a). It mainly comprises the Feda Graben in the south and the Breiflabb Graben (also known as the Jacqui Graben in the UK sector) in the northwest at the Norwegian–UK sector boundary (Gowers *et al.*, 1993; Erratt *et al.*, 1999) (Fig. 1a). To the northeast of the Norwegian Central Graben, across the Sørvestlandet High, lies the Norwegian–Danish Basin, and to the southwest lies the Mid North Sea High (Gowers & Sæbøe, 1985; Gowers *et al.*, 1993) (Fig. 1a). The tectono-stratigraphic evolution of the Central Graben was largely controlled by four main tectonic events: Permo–Triassic rifting, Middle Jurassic doming, Late Jurassic to Early Cretaceous rifting and inversion from the Middle Cretaceous to the Tertiary (e.g. Gowers *et al.*, 1993; Coward, 1995).

Permo-Triassic rifting

The Central Graben lies in part of the Northern Permian Basin that was formed in response to Early Middle Permian extension which is thought to have reactivated broadly NW–SE-striking Variscan thrust faults and inherited normal faults (Ziegler, 1982, 1990; Coward, 1995). Following deposition of the terrestrial Rotliegend Group, the Zechstein Supergroup was deposited after the Late Permian transgression (Ziegler, 1990; Hodgson *et al.*, 1992; Coward, 1995). In basinal areas, the Zechstein Supergroup is dominated by a thick halite, whereas towards basin margins and on intrabasin highs, carbonate or anhydrite dominate the Zechstein succession (Gowers & Sæbøe, 1985; Smith *et al.*, 1993; Clark *et al.*, 1998). These differences in lithology within the Zechstein Supergroup have a dramatic impact on its mobility and thus its influence on subsequent structural evolution (Gowers & Sæbøe, 1985; Clark *et al.*, 1998).

The reactivation of Permian extensional structures during Triassic rifting was accompanied by the deposition of fluvial sediments of the Skagerrak and Smithbank Formations and the initiation of widespread salt tectonics (e.g. salt diapirs and salt walls) in the Central Graben area (Hodgson *et al.*, 1992; Smith *et al.*, 1993; Erratt *et al.*, 1999; Stewart & Clark, 1999; Karlo *et al.*, 2014) (Fig. 2). In areas where the Zechstein Supergroup is relatively thin and/or contains a greater percentage of carbonate lithologies, salt tectonics was suppressed and the Triassic forms a sheet-like stratigraphic units (Clark *et al.*, 1998).

Early–Middle Jurassic doming

From Toarcian to Aalenian, the Norwegian Central Graben area was uplifted as part of the Middle North Sea Dome (Underhill & Partington, 1993). This uplift led to erosion of the Lower Jurassic and part of the Triassic successions in the Middle North Sea area, creating a regional unconformity termed the Mid-Cimmerian Unconformity (Ziegler, 1990; Underhill & Partington, 1993) (Fig. 2). Subsequent dome deflation and subsidence in the Middle Jurassic led to deposition of the Bryne Formation, which consists of fluvio-lacustrine and coastal plain deposits and is up to a few hundred metres thick (Ziegler, 1990; Hodgson *et al.*, 1992; Husmo *et al.*, 2002) (Fig. 2).

Late Jurassic-Early Cretaceous rifting

Jurassic rifting commenced in the Central Graben during the Middle Callovian under E–W extension (Erratt *et al.*, 1999; Stewart & Clark, 1999). The first pulse of rifting lasted to early Kimmeridgian times, and led to the

Basin Research published by International Association of Sedimentologists and European Association of Geoscientists and Engineers and John Wiley & Sons Ltd.

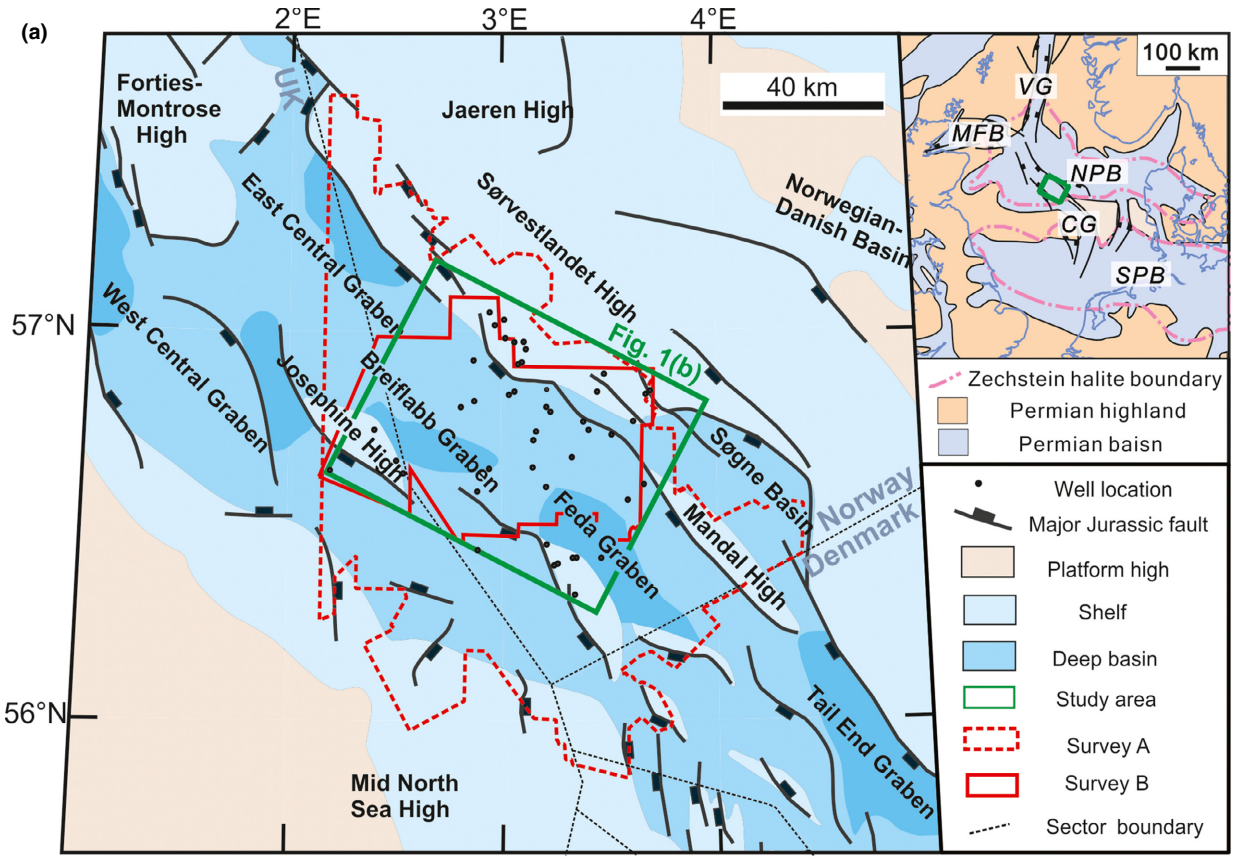

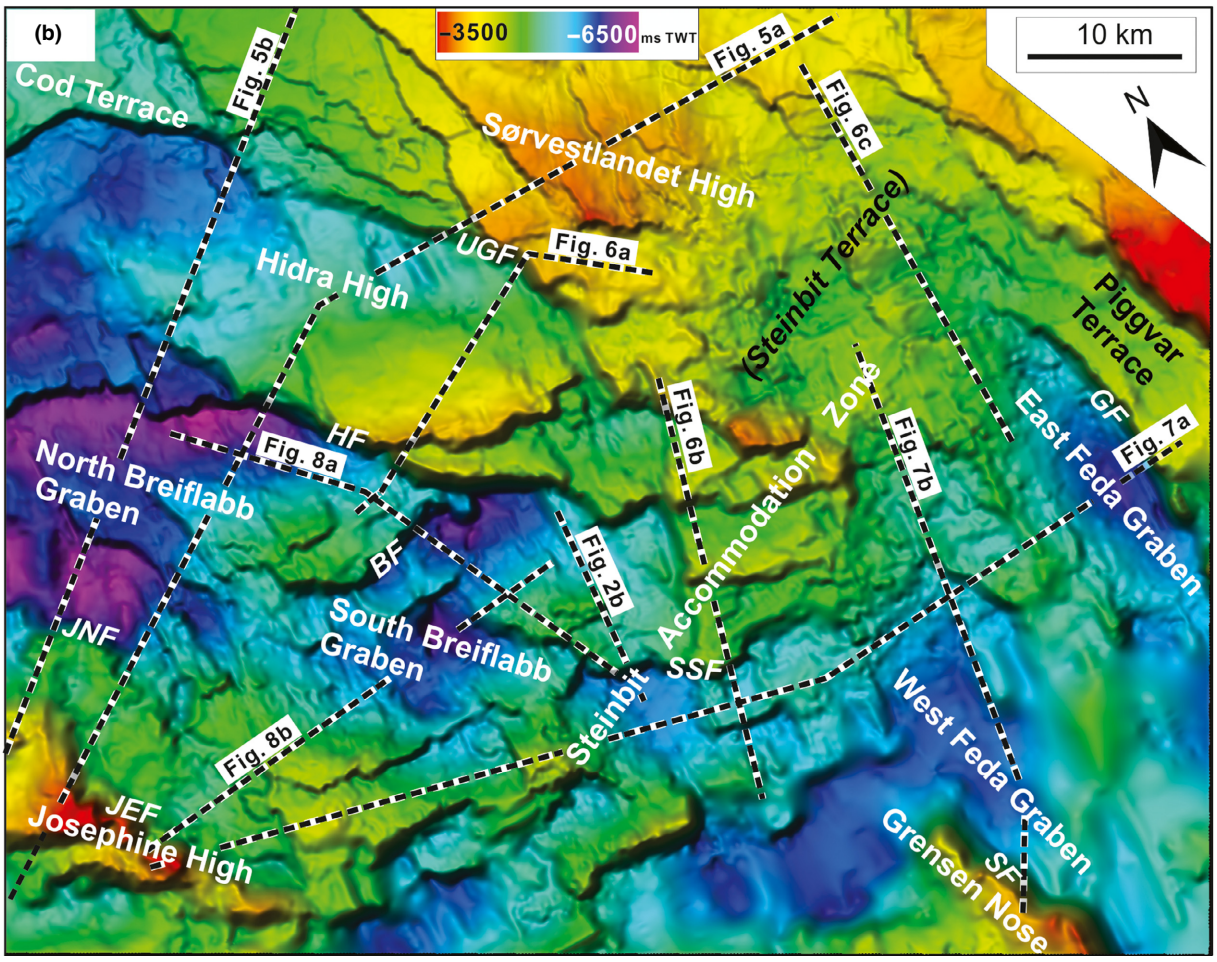

Basin Research published by International Association of Sedimentologists and European Association of Geoscientists and Engineers and John Wiley & Sons Ltd.

Fig. 1. (a) Simplified structural elements map of Late Jurassic Central Graben, North Sea showing location of the study area and distribution of wells and seismic data used in this study (modified after Erratt *et al.*, 1999 and Fraser *et al.*, 2003). The main structural elements are named. Inset shows the location of the Permian salt basins and the North Sea rift. NPB, North Permian Basin; SPB, South Permian Basin; VG, Viking Graben; MFB, Moray Firth Basin; CG, Central Graben (modified after Ziegler, 1990 and Duffy *et al.*, 2013). (b) Two-way travel-time (TWT) structure map illustrating the main structural elements defined on the base salt horizon (see Fig. 2). Note the shallow rift margin along the northeast and eastern margin of the study area and the Steinbit Accommodation Zone running east–west across the Central Graben, separating the Breiflabb grabens in the north from the Feda grabens in the south. The locations of Figures 2 and 5–8 are also shown. Fault abbreviations: UGF, Ula-Gyda Fault; HF, Hidra Fault; BF, Breiflabb Fault; JNF, Josephine North Fault; JEF, Josephine East Faut; SSF, Steinbit South Fault; GF, Gert Fault; SF, Skrubbe Fault.

establishment of marine conditions over most of the Norwegian Central Graben, except for local structural highs which remained emergent (e.g. Mandal High) (Ziegler, 1990; Gowers *et al.*, 1993; Fraser *et al.*, 2003). Shallow marine clastics (Ula Formation) followed by deep marine mudstones (Haugesund and Farsund Formations) were deposited in fault-controlled depocentres and in sub-basins that developed over collapsed salt walls (Hodgson *et al.*, 1992; Gowers *et al.*, 1993; Smith *et al.*, 1993; Mannie *et al.*, 2014; Wonham *et al.*, 2014). A second phase of rifting is interpreted to have occurred from late Kimmeridgian to early Volgian (Berriasian) and is associated with overall sediment starvation that led to the deposition of organic-rich mudstones (Mandal Formation) (Gowers *et al.*, 1993; Rattey & Hayward, 1993; Erratt *et al.*, 1999). Overall, the syn-rift interval has a total thickness of more than 3000 m in basin centres, thins towards basin margins and pinches out onto intra-basin highs where it is locally absent (Gowers & Sæbøe, 1985; Gowers *et al.*, 1993). Early Cretaceous post-rift sediments (Cromer Knoll Group) onlapped onto the Base Cretaceous Unconformity (BCU) and passively infilled remnant rift topography until regional inversion started in the Middle Cretaceous (Rawson & Riley, 1982; Rattey & Hayward, 1993).

Middle Cretaceous–Tertiary inversion

From mid-Albian times, the Central Graben went through multiple phases of inversion which have been related to intra-plate compression due to Alpine collision (Ziegler, 1990; Rattey & Hayward, 1993). The inversion caused uplift of syn-rift hanging wall depocentres, creating inversion anticlines, and led to compression of salt walls to form squeezed diapirs (Gowers & Sæbøe, 1985; Gowers *et al.*, 1993).

DATA SET AND METHODOLOGY

Data set

This study utilises two prestack, time-migrated, 3D reflection seismic surveys (Fig. 1a). Survey A covers the entire study area of roughly 4800 km^2 and has an inline and crossline spacing of 25 m with a record length of 6 s TWT (Fig. 1a). Survey B covers roughly 75% of the study area (*ca*. 3600 km^2) and has an inline and crossline spacing of 12.5 m with a record length of 8 s TWT (Fig. 1a). The data quality of both surveys is generally good to excellent within the interval of interest. The frequency of both seismic surveys in the interval of interest is between 20 and 30 Hz, giving a vertical seismic resolution of *ca*. 30–40 m based on an average seismic velocity of 3500 ms^{-1}.

Fifty-one wells that penetrate the Late Jurassic to Early Cretaceous rift succession, were used to calibrate seismic horizon interpretation (Fig. 1a). Of these wells, 38 wells extend to the base of the syn-rift succession, but only four of them penetrate beneath the Zechstein Supergroup. Furthermore, the majority of the wells are located on structural highs and along the margin of the Central Graben, so that very few wells are available in deeper, basinal areas. All wells have a conventional well-log suite (i.e. checkshots, gamma, sonic, density and neutron logs). Biostratigraphic information, from both proprietary reports and publicly available data from Norwegian Petroleum Directorate, was used to calibrate well tops and tie them to the seismic time-domain using checkshots, in order to constrain the ages of mapped seismic horizons.

Seismic stratigraphy

Stratal terminations, growth strata intervals and major changes of seismic facies were used to define key seismic horizons (Fig. 2). Four of these horizons that can be mapped regionally are used to divide the seismic stratigraphy into: (i) presalt, (ii) salt, (iii) pre-rift, (iv) syn-rift, and (v) post-rift (Fig. 2). The terms pre-, syn- and post-rift throughout this paper refers to the Late Jurassic to Early Cretaceous rift phase. A further four seismic horizons allow subdivision of the pre-rift, the syn-rift and the post-rift seismic strata into sub-units: pre-rift unit I and II, syn-rift unit 1 (SU1), 2 and 3, and post-rift unit I (Fig. 2).

The base salt horizon marks the top of a group of parallel, continuous, high amplitude reflectors and forms the boundary between presalt and salt (Fig. 2). The top salt horizon caps the Zechstein Supergroup and is locally a high amplitude (peak) reflector, but its continuity deteriorates dramatically on the edge of salt walls and diapirs where it is steeply inclined (Fig. 2). The base syn-rift horizon is marked by local onlap above and truncation below and also delineates the base of growth packages where syn-rift stratal wedges are present in the hanging wall of normal faults or adjacent to salt structures.

Basin Research published by International Association of Sedimentologists and European Association of Geoscientists and Engineers and John Wiley & Sons Ltd.

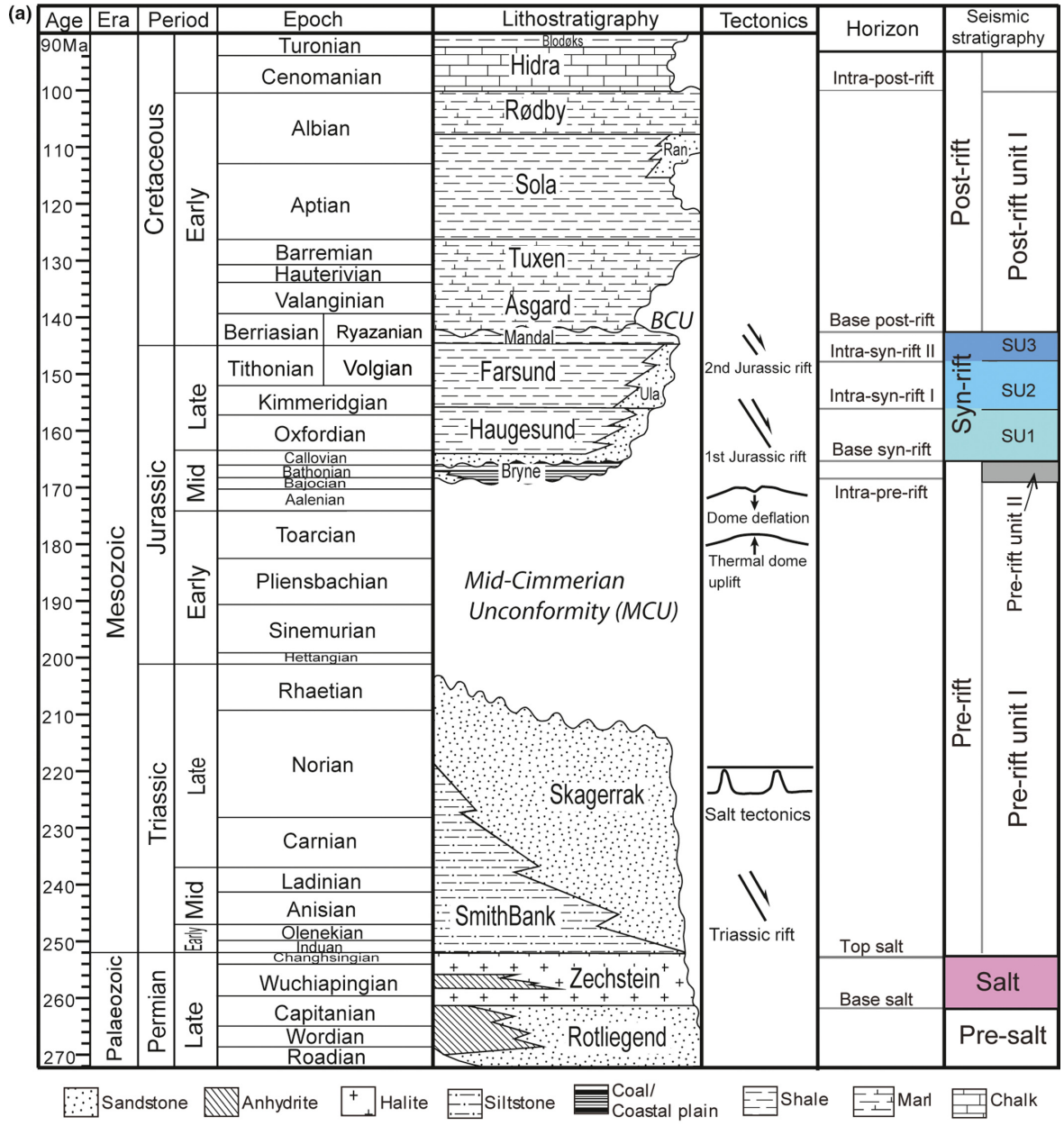

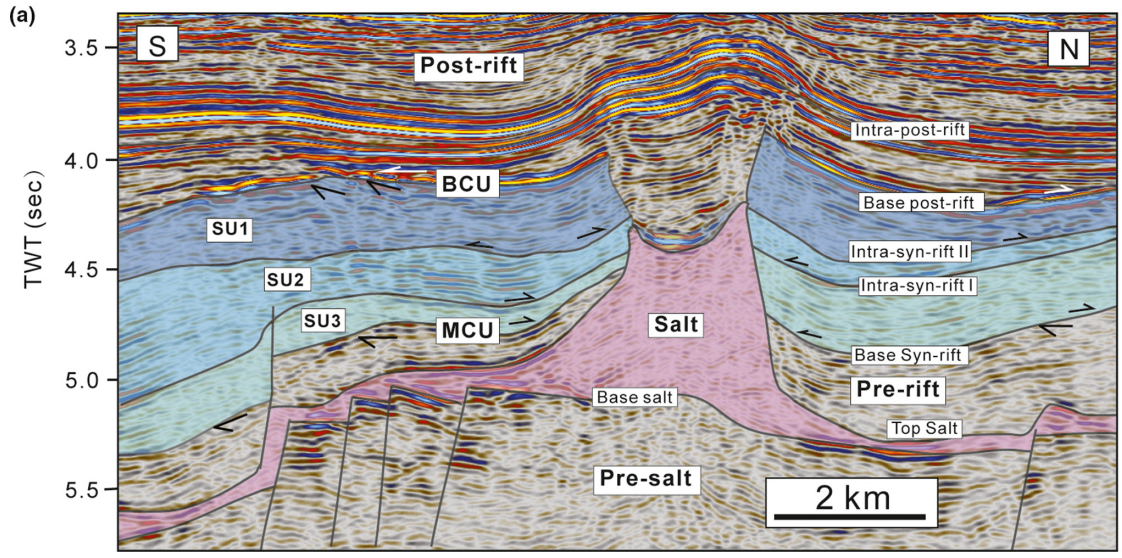

Fig. 2. (a) Simplified Late Permian to Middle Cretaceous stratigraphy of the Central Graben and main tectonic events (modified after Gowers *et al.*, 1993; Underhill & Partington, 1993; Rattey & Hayward, 1993; Gradstein *et al.*, 2010). The main seismic horizons mapped and associated seismic intervals studied are indicated on the righthand side. (b) A representative seismic section from the Norwegian Central Graben. The seismic data is processed to zero phase with red colour indicating a peak. Note the Mid Cimmerian Unconformity (MCU) and Base Cretaceous Unconformity (BCU).

Truncation beneath the base syn-rift is locally developed on structural highs, or where the Middle Jurassic is thin to absent such that the base syn-rift is composite with the Mid-Cimmerian Unconformity (Fig. 2). The base post-rift horizon forms the top of the syn-rift unit, separating it from the overlying post-rift strata (Fig. 2). This horizon has been widely referred to as the BCU or Late Cimmerian Unconformity (see the discussion in Rattey & Hayward, 1993). The horizon is generally a strong reflector with local truncations below and onlap above. The high amplitude and good continuity of the reflector are due to a change in lithology from clay-rich mudstone below to marls above.

Within the syn-rift seismic strata, the intra syn-rift I and intra syn-rift II horizons subdivide the Late Jurassic to Early Cretaceous syn-rift interval into three sub-units: syn-rift unit 1 (SU1), syn-rift unit 2 (SU2) and syn-rift unit 3 (SU3) (Fig. 2). Typically, these intra-syn-rift reflectors have low to moderate amplitude and continuity, and are marked by local onlap of overlying reflectors (Fig. 2). Well-to-seismic ties suggest that the intra syn-rift I and intra syn-rift II horizons are middle Kimmeridgian and middle Volgian in age respectively.

Two horizons were mapped within the pre-rift and post-rift seismic strata. The intra-pre-rift horizon is a locally mapped horizon with strong to moderate amplitude, marking the base of Bryne Formation (Fig. 2). The Bryne Formation tends to be very thin, usually a few metres to a few tens of metres thick and this is often at, or below seismic resolution. Mapping of this horizon relied heavily on well calibration and is only possible where the Bryne Formation is relatively thick. Within the post-rift interval, the intra post-rift horizon is a high amplitude, high continuity reflector, marking the transition from deposition of marl to chalk during late Albian (Fig. 2).

Two-way travel-time (TWT) structure maps, seismic profiles and isochron maps were used to describe the present-day structural style within different seismic units, and to determine the timing of activity on different structures. Post-rift inversion was noted when interpreting the present-day structural geometry and was qualitatively removed by flattening on post-rift reflectors, but no restoration was performed. Having performed the study in the time domain, some geometric distortion is expected, particularly adjacent to faults and/or the flanks of salt-related structures. However, by integrating the observations of seismic stratigraphy and the isochron map of syn-rift units, a high confidence can be maintained to construct the relationship among sub-salt faults, pre-rift salt-related structures, and syn-rift depocentres.

PRE-RIFT STRUCTURAL STYLE OF THE LATE JURASSIC NORWEGIAN CENTRAL GRABEN

This section describes the present-day structural style of the sub-salt faults and the pre-rift salt-related structures. The sub-salt structure of the study area is best illustrated by the time-structure map of the base salt horizon (Figs 1b and 3). Isochron maps (Fig. 4) were used to define the present-day distribution of the salt and the pre-rift strata, thereby constraining the pre-rift salt-related structural style. The nomenclature of the main structural elements broadly follows that of Gowers & Sæbøe (1985) and Gowers *et al.* (1993), but has been changed locally, because the boundaries between some of the structural elements are more clearly defined in the 3D seismic data set available in this study. Major normal faults not previously named are named here on the basis of their geographic location. The study area can be divided into three structural domains based on the present-day TWT-elevation of the base salt horizon and the geometry and throws of the sub-salt faults: (i) *rift margin* – comprising the Cod Terrace, Sørvestlandet High and Steinbit Terrace along the eastern flank of the graben, (ii) *rift axis* – comprising the North and South Brieflabb Grabens and Hidra High in the north and East and West Feda Grabens in the south, and (iii) *Steinbit Accommodation Zone* – separating the Brieflabb and Feda grabens along the rift axis and extending eastward into the Steinbit Terrace (Fig. 1b).

Sub-salt structure

The base salt horizon is highly faulted, with an average fault spacing of 3–5 km (Figs 1b and 3a). The sub-salt faults can be roughly grouped into three sets based on their strike: N–S, NW–SE and E–W to ESE–WNW (Fig. 3a). The third set, that is, the E–W to ESE–WNW fault set, is the most common in the study area (Fig. 3c), but it contains few major large throw faults (Fig. 1b).

Rift margin

The Sørvestlandet High is a 25-km long and 10–15-km wide NW–SE-trending structural high located along the northeast margin of the rift (Fig. 1b). It has a present-day elevation ranging from 3.8 s TWT in the southwest to 4.5 s TWT in the northeast and extends to the north and east outside the study area (Fig. 1b). The Sørvestlandet High bounds the Cod Terrace in the northwest and the Steinbit Terrace in the southeast (Fig. 1b). A major

Basin Research published by International Association of Sedimentologists and European Association of Geoscientists and Engineers and John Wiley & Sons Ltd.

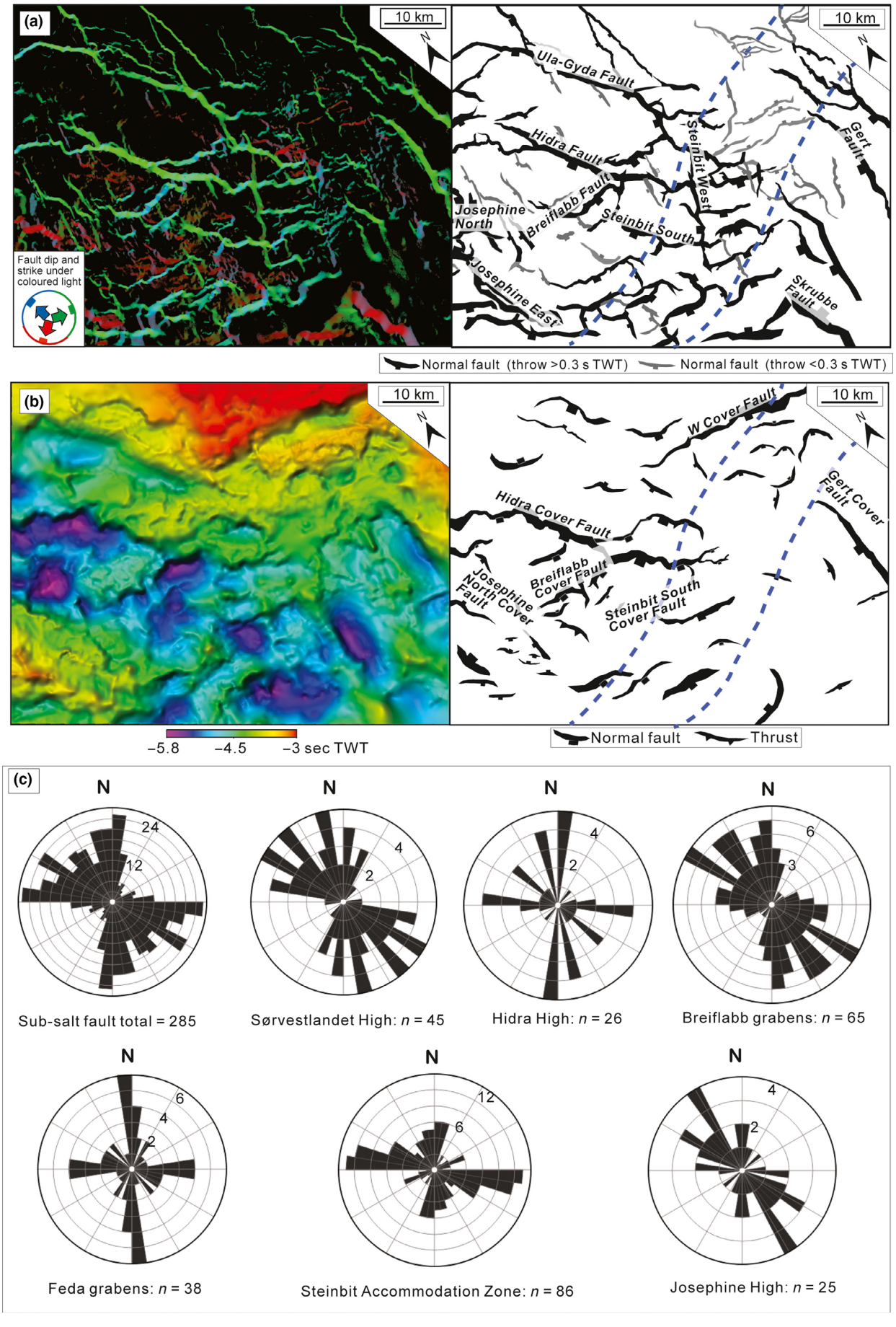

Fig. 3. Sub-salt and supra-salt fault maps. (a) two-way travel-time (TWT) structure map of base salt horizon highlighting major sub-salt faults (left) and simplified interpretation (right). Different fault-dip directions are highlighted in colour: green, dipping W and SW; blue, dipping S and SE; red, dipping E and NE. (b) TWT structure map of base syn-rift horizon showing the supra-salt faults (left) and simplified interpretation (right). Note decreased number of supra-salt faults compared to sub-salt faults. (c) Sub-salt fault rose diagram indicating variation in strike of the main faults. The two diagonal blue dashed lines in (a) and (b) delineate the Steinbit Accommodation Zone.

segmented normal fault, the Ula-Gyda Fault, bounds the western side of the high. Internally, N–S-striking and ESE–WNW-striking faults dissect the high, with maximum faults throws ≤300 ms TWT and an average spacing of 5 km (Fig. 3a). The Ula-Gyda Fault is approximately 35 km long, generally strikes NW–SE and dips to the SW (Fig. 3a). The maximum throw along Ula-Gyda fault is over 1200 ms TWT on the base salt horizon, and occurs near the centre of the fault (Fig. 5a). The southeastern part of the Ula-Gyda Fault changes to strike NNW–SSE and branches into three NW–SE-striking splay faults that gradually tip out into the Steinbit Terrace to the southeast (Figs 1b and 3a).

Rift axis

The rift axis is composed of large tilted fault blocks that are 10–15-km wide and 20–40-km long, with hanging wall lows ≥5.8 s TWT, and includes the Hidra High, the Feda Graben and the Breiflabb Graben (Fig. 1b). The Hidra High is located immediately west of the rift margin and is a major fault block, 40-km long and 15-km wide (Fig. 1b). It is bounded to the southwest by the Hidra Fault and to the northeast by the Ula-Gyda Fault (Fig. 5). The SW-dipping Hidra Fault is *ca*. 50-km long, generally NW–SE-striking, and composed of three main segments (Fig. 3a). It has a maximum throw of *ca*. 2000 ms TWT near the boundary between the middle and eastern segments (Fig. 6a).The Hidra High fault block is strongly tilted towards the northeast, with the base salt horizon deepening from *ca*. 4.0 s TWT in the immediate footwall of the Hidra Fault, to *ca*. 5.8 s TWT in the immediate hanging wall of the Ula-Gyda Fault, some 20 km to the northeast. Internally, the Hidra High is dissected by E–W and N–S-striking minor faults <5 km in length (Fig. 3c).

The Feda Graben as defined by Gowers *et al.* (1993; their fig. 3) includes the large area from the Gert Fault in the east to the Josephine High in the west, and the Steinbit Terrace in the north and the Grensen Nose in the south-southwest (Figs 1b and 3a). More recent 3D seismic data reveal that the sub-salt structural style of the area is complex, with fundamental differences between east and west (Fig. 1b). In the east, the Feda Graben is characterised by major N–S-striking, fault-bounded blocks, tens of kilometres long and wide. In contrast, in the west, it comprises a series of sub-basins that are typically <10 km in length and width, and bounded by faults with varied strikes (Fig. 1b). Based on these differences in structural style, the area previously defined as the Feda Graben can be divided into three distinct structural elements (Fig. 1b): (i) the Feda Graben in the east; (ii) the South Breiflabb Graben in the west, and (iii) the Steinbit Accommodation Zone separating the Feda Graben and the South Breiflabb Graben.

The Feda Graben, as defined here, is bounded by the Gert Fault in the east and Skrubbe Fault in the west (Figs 1b and 3a). Within the Feda Graben, a 5-km-wide, 20-km-long horst extends southward from the Steinbit Accommodation Zone, and divides the Feda Graben into two sub-basins, each >20 km long and >10 km wide, termed the East Feda Graben and the West Feda Graben (Fig. 1b). The base salt horizon in the East Feda Graben occurs at 5.8 s TWT in the hanging wall of the N–S-striking, W-dipping Gert Fault and shallows to 5 s TWT on the horst (Fig. 7a). The Gert Fault is >20 km long, and has a maximum throw at *ca*. 1600 ms TWT in the study area (Fig. 7a). To the west of the horst, the West Feda Graben is separated from the Grensen Nose to the west by the N–S-striking, E-dipping Skrubbe Fault (Fig. 7b). The Skrubbe Fault is >10 km long and has maximum throw of *ca*. 1800 ms TWT at the base salt horizon. Within the West Feda Graben, E–W-striking faults dominate and have maximum fault throws <300 ms TWT (Fig. 3c).

The Breiflabb Graben forms the present-day deep axial part of the Central Graben, with the base salt horizon at >6 s TWT in the east of the study area (Fig. 1b). The graben is 20 km wide and 40 km long, and is bounded by the Hidra Fault in the northeast, the Steinbit West Fault in the south and the Josephine North Fault in the southwest (Fig. 3a). Previous interpretation treats the Breiflabb Graben as a uniform basin (Gowers *et al.*, 1993; their fig. 3). More recent 3D seismic data indicates that a curved 10-km-long, E–W-striking fault with *ca*. 900 ms TWT maximum throw, here termed the Breiflabb Fault, abuts against the eastern part of the Hidra Fault, and divides the area into northern and southern sub-basins – here termed the North Breiflabb Graben and the South Breiflabb Graben (Figs 1b, 3a and 8a). The North Breiflabb Graben is tilted to the north and is internally dissected by 5–10-km-long N–S-striking faults, with average spacing <5 km (Figs 3a and 8a). Further west, the 8-km-long NW–SE-striking, NE-dipping Josephine North Fault bounds the western side of the North Breiflabb Graben, separating it from the Josephine High. The maximum throw on the Josephine North Fault is >1400 ms TWT (Fig. 5b). The South Breiflabb Graben is *ca*. 20 km long and 10 km wide and tilted towards the

Basin Research published by International Association of Sedimentologists and European Association of Geoscientists and Engineers and John Wiley & Sons Ltd.

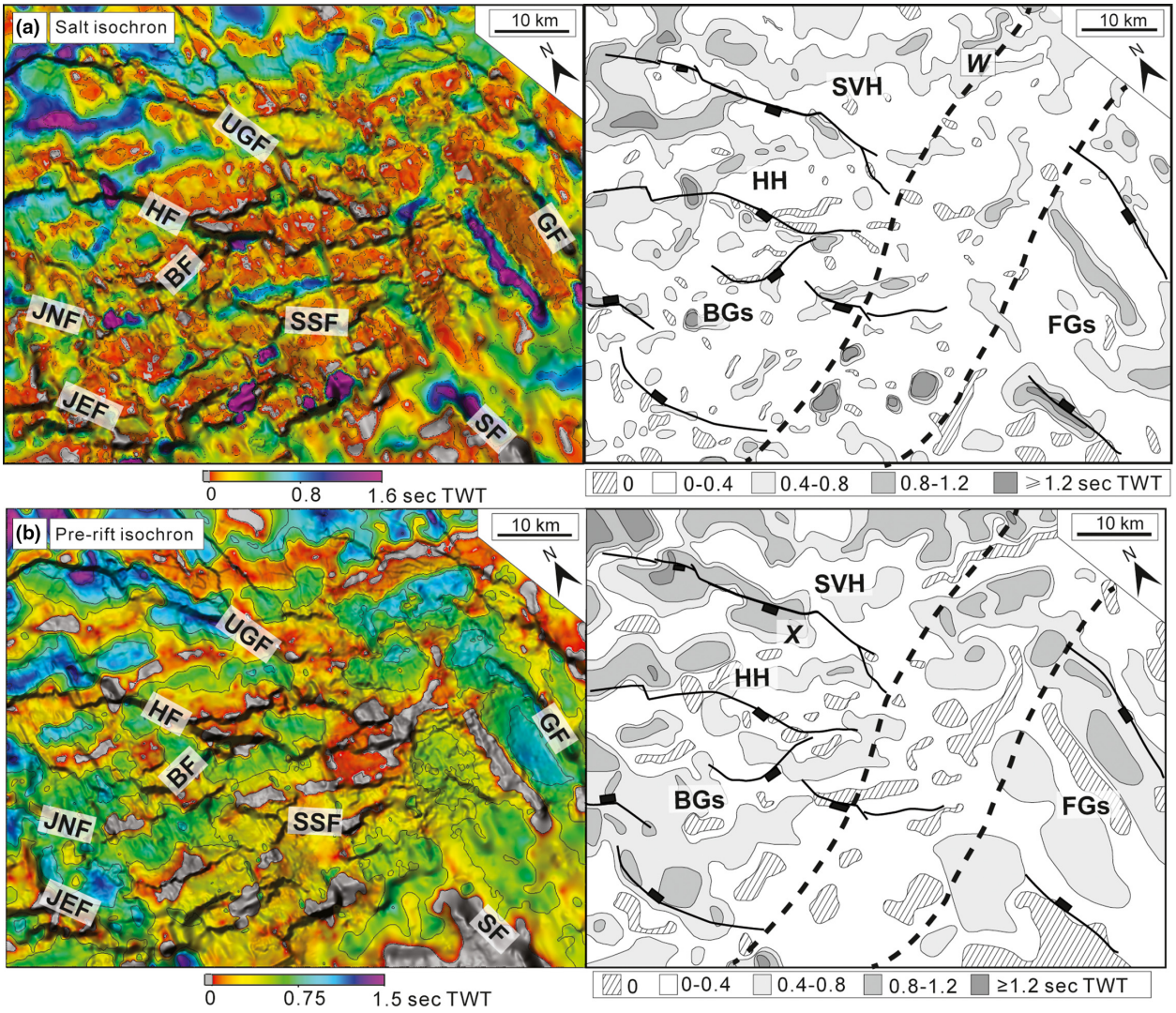

Fig. 4. Isochron maps of salt and pre-rift seismic units. (a) Isochron map of salt overlain two-way travel-time (TWT) structure map of base salt horizon (left) and simplified salt isochron map with main faults (right). The colour bar highlights the thick (blue) and thin (orange) salt. (b) Pre-rift isochron map overlain TWT structure map of base salt horizon (left) and the simplified pre-rift isochron map with main faults (right). Fault abbreviations: UGF, Ula-Gyda Fault; HF, Hidra Fault; BF, Breiflabb Fault; JNF, Josephine North Fault; JEF, Josephine East Faut; SSF, Steinbit South Fault; GF, Gert Fault; SF, Skrubbe Fault. Area abbreviations: SVH, Sørvestlandet High; HH, Hidra High; BGs, Breiflabb grabens; FDs, Feda grabens. The two diagonal dashed lines in (a) and (b) delineate the Steinbit Accommodation Zone. W and X relate to description in the main text.

northeast, with the base salt horizon deepening from *ca*. 4 s TWT near the Josephine High to >6 s TWT in the hanging wall of Breiflabb Fault (Fig. 1b).

Steinbit Accommodation Zone

A zone 15–20 km wide characterised by a relatively shallow base salt horizon (4.5–5.5 s TWT) crosses the Norwegian Central Graben, separating the large rift-axis fault blocks of the Hidra High and the Breiflabb Graben in the northwest from the Feda Graben in the southeast (Fig. 1b). We term this structural high the Steinbit Accommodation Zone, named after the Steinbit Terrace of Gowers *et al.* (1993), from which it extends westward across the Norwegian Central Graben (Fig. 1b).

Within the accommodation zone, the average fault spacing and maximum throw increase from 2 to 3 km and <300 ms TWT, respectively, in the east (Steinbit Terrace) to 5–10 km and >800 ms TWT in the west, and the depth of base salt horizon deepens from 4.5–5 s TWT to 5–5.5 s TWT towards the west (Fig. 1b). The largest fault in the accommodation zone is the Steinbit South Fault, a curved, E–W- to NW–SE-striking, S to SW dipping fault with maximum throw of *ca*. 900 ms TWT (Fig. 6b). It is about 18 km long and tips out into the South Breiflabb Graben (Fig. 3a). The boundary between the accommodation zone and the South Breiflabb Graben is marked by the northeast part of the Steinbit West Fault, a 16-km-long NNE–SSW-striking, WNW-dipping fault with maximum throw of *ca*. 800 ms TWT and

Basin Research published by International Association of Sedimentologists and European Association of Geoscientists and Engineers and John Wiley & Sons Ltd.

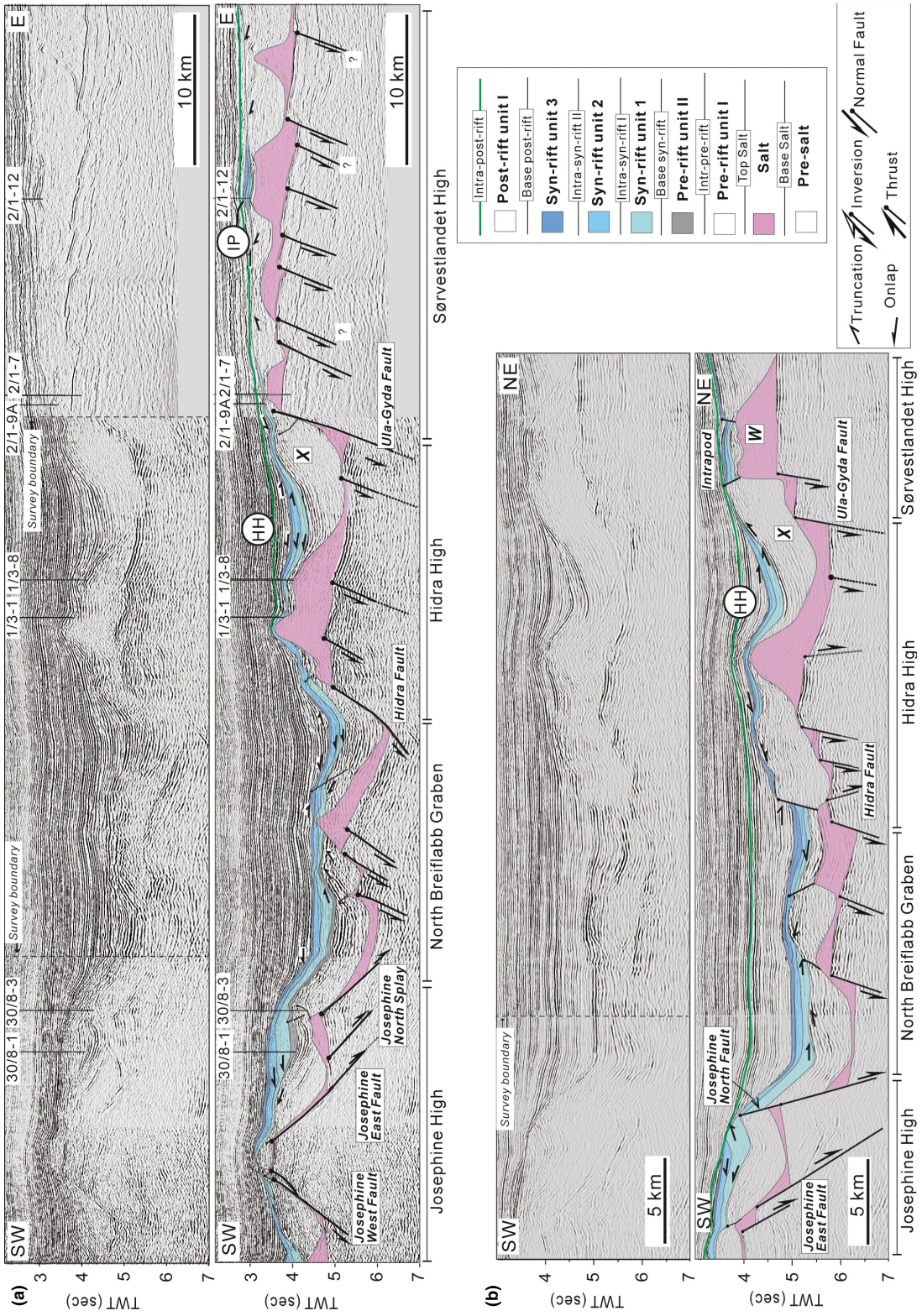

Fig. 5. Representative seismic sections (above) and interpretation (below) illustrating the structural style and syn-rift depocentre geometry from the northern segment of the Central Graben. (a) E–W section from the Sørvestlandet High to the Josephine High, crossing the Hidra High and North Brieflabb Graben. Note thick pre-rift minibasins and elongate, connected salt walls and the contrast between complex sub-salt fault pattern and relatively simple supra-salt faults. (b) NE–SW section across the Sørvestlandet High, Hidra High, North Brieflabb Graben and Josephine High. Note the rotated minibasin (X) and overlying synclinal syn-rift depocentre developed over the Ula-Gyda Fault, and the thick early post-rift succession in the North Breiflabb Graben. HH, IP and X relate to description in the text. See Fig. 1b for location. Seismic data courtesy of CGG and PGS.

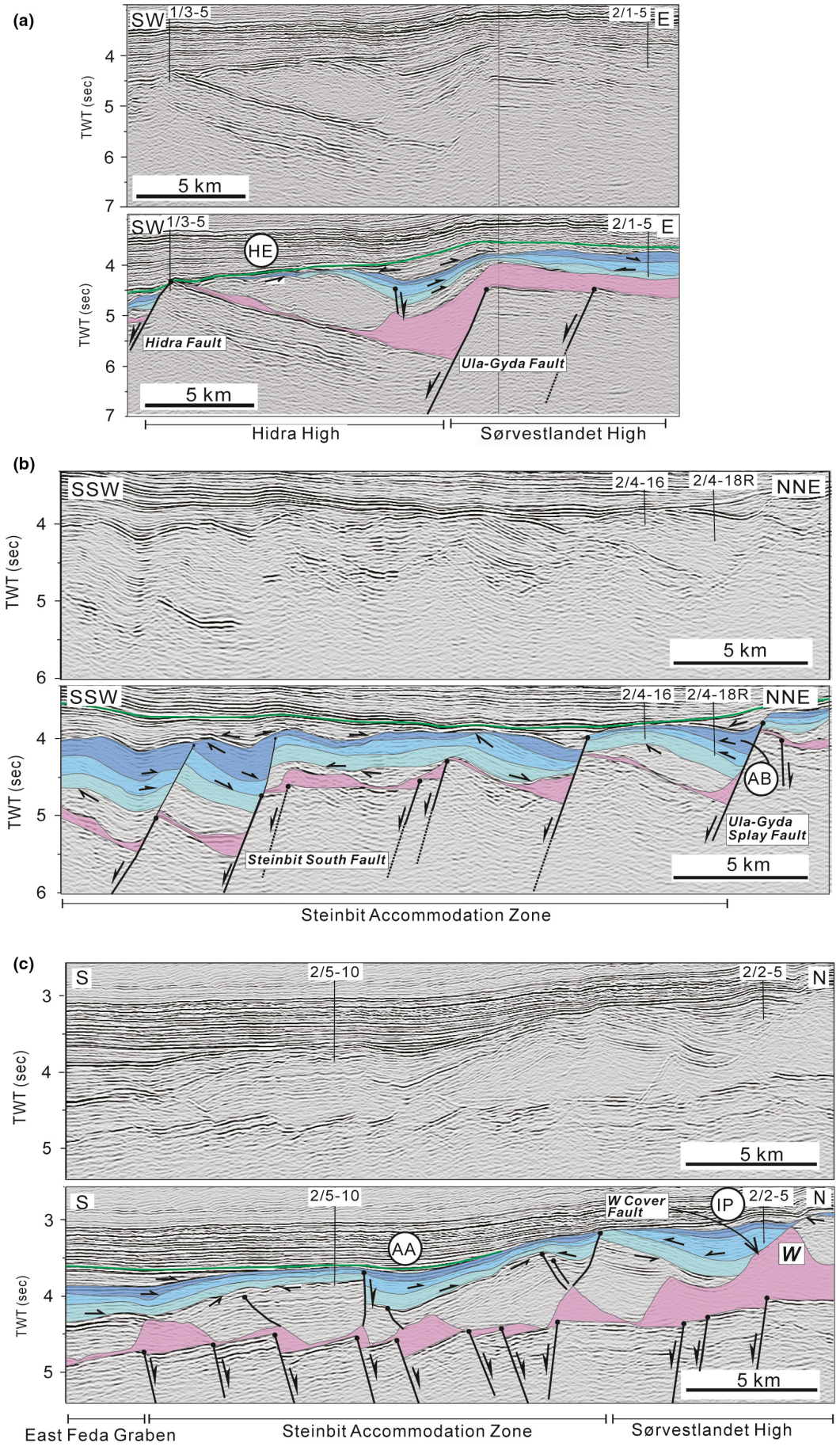

Basin Research published by International Association of Sedimentologists and European Association of Geoscientists and Engineers and John Wiley & Sons Ltd.

Fig. 6. Seismic sections (above) and interpretations (below) illustrating the variation in structural style and syn-rift depocentre geometry between major fault blocks of the rift segments and the Steinbit Accommodation Zone. (a) E-SW section across the Sørvestlandet High and Hidra High highlighting the major sub-salt normal faults (Hidra and Ula-Gyda Faults) and structural style from the southern end of the northern rift segment. (b) and (c) Sections across the Sørvestlandet High and Steinbit Accommodation Zone illustrating the typical sub-salt faulting and pre-rift deformation. Note the syn-rift depocentres are largely decoupled from sub-salt faulting. HE, AB, AA and IP relate to description in the text. See Fig. 5 for legend; Fig. 1b for location. Seismic data courtesy of CGG.

the middle part of the Steinbit South Fault (Figs 3a and 7a).

Pre-rift salt-tectonic structural style

The present-day isochron map of the salt unit displays marked thickness changes as the average salt thickness decreases from north to south and has an antithetic thickness relationship with the isochron map of the pre-rift strata (Fig. 4). There are three structural styles in the pre-rift unit in the study area. Two of them reflect the degree of salt tectonics affecting the pre-rift succession: one comprises connected elongate salt walls and intervening thick minibasins, whereas the second is characterised by isolated salt diapirs separated by thin minibasins. The third structural style comprises pre-rift strata that has a sheet-like geometry with thin to moderate salt thickness and rare salt diapirs.

Rift margin

In the rift margin area of the Sørvestlandet High, elongate, connected salt walls and thick minibasins dominate the pre-rift structure (Fig. 4a). Both the salt walls and the intervening minibasins are >800 ms TWT thick and >5 km wide, and mainly E–W striking. The strike of these salt-tectonic structures is notably different from the broadly N–S-striking sub-salt normal faults in this area (Fig. 1b). The salt walls are connected to each other, forming a complex network that extends for tens of kilometres along strike (Fig. 4a). For example, the largest salt wall (W in Fig. 5b) extends along strike for over 50 km from northwest of the Ula-Gyda Fault to the northeast of the study area, near the boundary between the Sørvestlandet High and the Steinbit Accommodation Zone (W in Figs 4a and 6c). The minibasins surrounding salt wall W mainly contain Triassic sediments up to 1000 ms TWT thick (Fig. 5). Within the Triassic succession, internal growth wedges are locally observed, suggesting complex salt tectonics during the Triassic (Karlo *et al.*, 2014). In map view, these minibasins are typically 5–10 km wide and 6–20 km long (Fig. 4b).

Rift axis

In the rift axis, all three pre-rift structural styles can be found (Fig. 4b). The elongate, connected salt walls and thick minibasins extend from the Sørvestlandet High across the Hidra High, with the present-day thickness of the minibasins reduced due to the footwall uplift and Late Jurassic/Early Cretaceous erosion (Fig. 6a). Further west, in the Breiflabb Graben, the elongate salt walls are replaced by isolated salt diapirs surrounded by thin minibasins (Fig. 4). For example, in the South Breiflabb Graben, salt diapirs rise up to 600 ms TWT above the base salt horizon and the minibasins are typically 600–800 ms TWT thick, and 4–6 km wide (Fig. 8b).

In the Feda Graben, the pre-rift strata have a more sheet-like, layer-cake geometry, with thin to moderate salt thickness, typically <500 ms TWT (Fig. 7). This structural style is best illustrated by the West Feda Graben (Fig. 7b). Here, the gently folded pre-rift is 300–500 ms TWT thick and extends laterally, with little thickness variation, for over 30 km in a north–south direction (Fig. 7b). Internal reflectors in the pre-rift strata are parallel to sub-parallel, indicating little or no salt tectonics in the area during pre-rift times (Fig. 7b). However, in the East Feda Graben, thinning of pre-rift strata, from 800 ms TWT to 200–400 ms TWT across the Gert Fault, suggests salt tectonics, presumably due to local fault activity (Figs 4b and 7a).

Steinbit Accommodation Zone

Within the Steinbit Accommodation Zone, the structural style of the pre-rift changes from east to west. The eastern part of the accommodation zone is characterised by salt walls and diapirs and minibasins (Fig. 6c). In the middle of the accommodation zone, the pre-rift structures are also salt walls and diapirs, but the pre-rift minibasins are much thinner, typically 200–500 ms TWT (Fig. 6b). In the western part of the accommodation zone, the pre-rift unit has a sheet-like geometry (Fig. 7a). Notably, a salt dome, in excess of 800 ms TWT thick, lies against the immediate hanging wall of the Steinbit West Fault (Fig. 7a). Reflectors within the pre-rift are sub-parallel, but are folded by the salt dome indicating that the salt dome formed after deposition (Fig. 7a). Similar salt domes are abundant in the study area; in most cases they, too, are related to salt mobilisation in response to rifting.

LATE JURASSIC SYN-RIFT TECTONOSTRATIGRAPHY OF THE NORWEGIAN CENTRAL GRABEN

Overall, the Late Jurassic syn-rift succession thickens from north to south across the study area, displaying

Basin Research published by International Association of Sedimentologists and European Association of Geoscientists and Engineers and John Wiley & Sons Ltd.

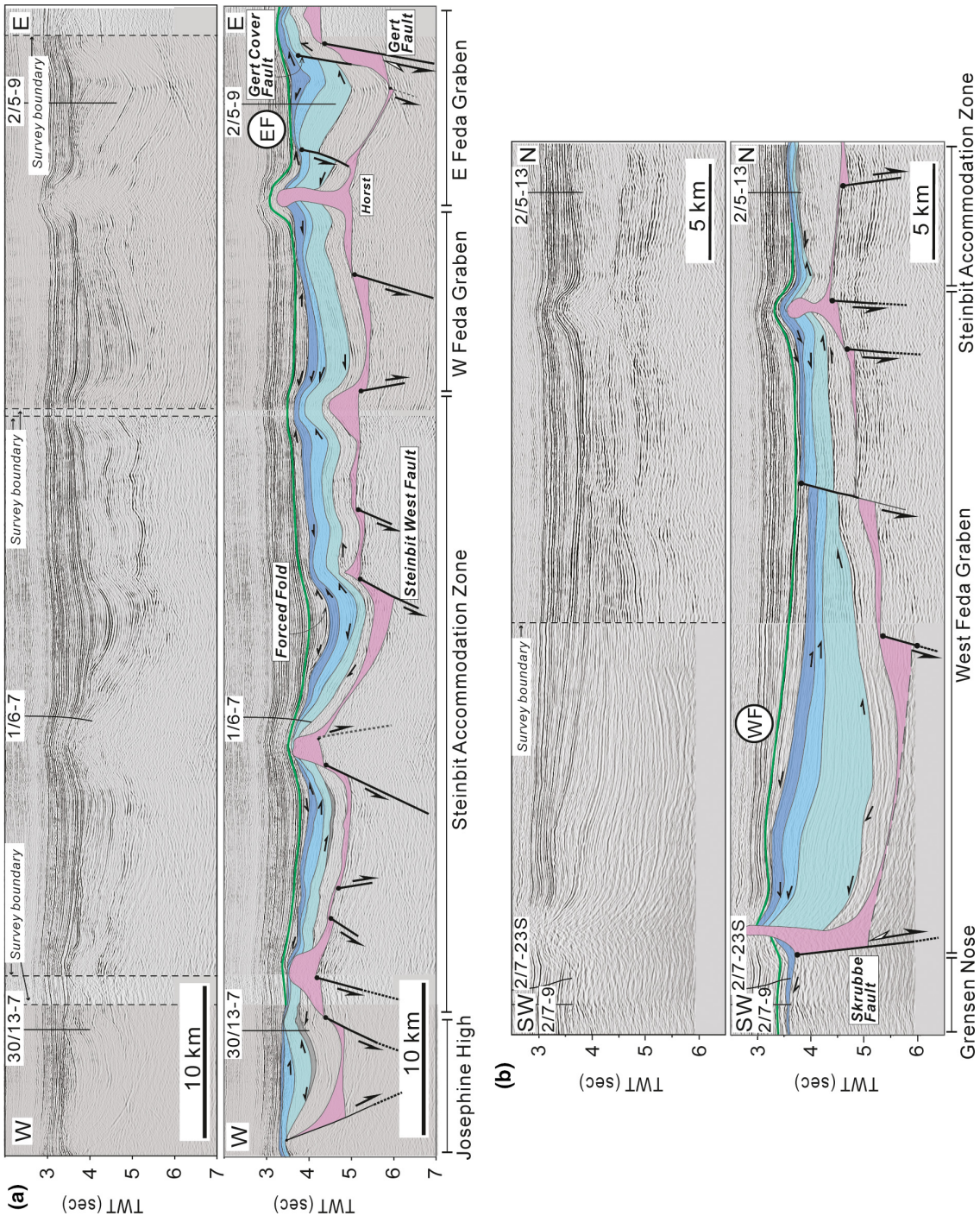

Fig. 7. Seismic sections (above) and interpretations (below) illustrating the structural style and syn-rift depocentre geometry of the Steinbit Accommodation Zone and southern rift segment. (a) E–SW section across the Feda grabens and eastern part of the Steinbit Accommodation Zone. Note the wide presence of folding and lack of faulting in the supra-salt strata. (b) N–S section across the Steinbit Accommodation Zone, West Feda Graben and Grensen Nose. Note the gradual thickness change in prerift strata. EF and WF relate to description in the text. See Fig. 5 for legend; Fig. 1b for location. Seismic data courtesy of CGG and PGS.

rapid thickness changes across normal faults, folds and salt-cored structures (Fig. 9). On the rift margin and on the crest of salt diapirs and large fault blocks, the syn-rift succession is locally absent or below seismic resolution (e.g. HE in Fig. 9a). In other structural locations, the syn-rift unit reaches thicknesses of up to 1.8 s TWT, for example, in the Feda Graben in the south of the study area (Fig. 9a). In the following subsections we describe and interpret representative examples of syn-rift depocentres and their relationship with sub-salt normal faults and pre-rift salt-related structures. For ease of comparison among different structures, we present these using the three structural domains recognised from the sub-salt fault network, namely the rift margin, rift axis and rift accommodation zone (Figs 1b and 9a).

Rift margin

Syn-rift depocentres along the rift margin are elongate, typically 10–15 km long, and relatively narrow, 5–8 km wide, and contain up to 0.8-s-TWT thick syn-rift succession (e.g. IP in Figs 5a and 9a). These depocentres (termed interpods by Hodgson *et al.*, 1992) occur above salt walls, and are flanked by thick pre-rift minibasins (Figs 5a and 9a). Typically these syn-rift depocentres are decoupled from sub-salt normal faults (Fig. 5a, b). In cross-sections they have a symmetrical geometry, and the individual syn-rift units, SU1 to SU3, are typically 50–150 ms TWT thick (Fig. 10). A notable exception to these characteristics occurs on the eastern part of salt wall W (Fig. 6c), at the boundary between the rift margin and the Steinbit Accommodation Zone. Here, the syn-rift growth wedge has a strongly asymmetrical, northward-thickening, wedge-shaped geometry, showing significant expansion of syn-rift unit SU2 towards the salt wall, where it reaches up to 400 ms TWT in thickness. This suggests that the pre-rift minibasin beneath the syn-rift depocentre rotated strongly during SU2 times, most probably related to salt mobilisation within the accommodation zone (Figs 6c and 10b).

Rift axis

Syn-rift depocentres along the rift axis show significant variability in their location, geometry and thickness (Figs 9 and 10). Major sub-salt normal faults play an important role in controlling the location of the depocentres along the rift axis and their variability is strongly influenced by how the sub-salt normal faults interact with pre-rift salt-related structures.

The syn-rift depocentre of the West Feda Graben (WF in Fig. 9a) has a relatively simple half-graben geometry, similar to classical half-graben geometries in salt-free rifts. The depocentre is over 20 km long and 10 km wide, and syn-rift strata thicken into the immediate hanging wall of the Skrubbe Fault, where they reach up to 1.8 s TWT in thickness (Figs 7b and 9a). Within the syn-rift succession, SU1 has a pronounced wedge-shaped geometry and is the thickest syn-rift unit, reaching up to 1.2 s TWT in the immediate hanging wall of the Skrubbe Fault. SU2 and SU3, in comparison, are relatively thin, with an average thickness of 0.2 and 0.3 s TWT, respectively, and display thinning and onlap towards the diapir in the immediate hanging wall of the Skrubbe Fault (Fig. 7b). In contrast, in the footwall of the Skrubbe Fault, SU1 and SU2 are absent and SU3 $\leq$0.1 s TWT in thickness (Figs 7b and 10). The Skrubbe Fault is thus interpreted to have been active early during Late Jurassic rifting, causing uplift and erosion in its footwall and generating space to allow deposition and preservation of the early syn-rift wedge in its hanging wall (e.g. SU1). The syn-rift stratal geometries in the immediate hanging wall of the Skrubbe Fault are complicated by salt diapirism which, based on the thinning and onlap relationships of SU2 and SU3, was only active later in the rift evolution (Figs 7b and 11b).

In the East Feda Graben (EF in Fig. 9a), a major elongate growth wedge, 20 km long and 8 km wide, with up to 1.8 s TWT of syn-rift strata, is developed in the immediate hanging wall of the Gert Fault (Fig. 7a). Within the growth wedge, SU1 is thickest 2–3 km into the hanging wall of the Gert Fault, where it is up to 0.6 s TWT thick, and thins towards the fault and into the footwall where it is only approximately 0.3 s TWT thick (Figs 7a and 10a). In contrast, SU2 is thickest in the immediate hanging wall of the Gert Fault and thins abruptly across the fault onto the footwall (Fig. 7a). Such thinning and thickening relationships are typical of upward propagation of normal faults and forced folding above fault tips (e.g. Withjack *et al.*, 1990; Schlische, 1995; Gawthorpe *et al.*, 1997). The thickness variations within the syn-rift units suggest that the Gert Fault was active throughout rift evolution, but the style of deformation changed progressively. During SU1 times, the supra-salt structure was characterised by a forced fold above an upward-propagating sub-salt normal fault, and the depocentre was located 2–3 km into the hanging wall of the Gert Fault. By SU2 times, however, a fault had nucleated in the pre-rift, shifting the depocentre eastward into its immediate hanging wall (Fig. 7a). This supra-salt segment of the Gert Fault was and still remains physically decoupled from the sub-salt segment of the Gert Fault (Fig. 7a).

The South Breiflabb Graben is bounded by the Breiflabb Fault and the Steinbit South Fault and contains two distinct syn-rift depocentres, each 10 km long and 5 km wide, with over 1.0 s TWT thickness, that are (B1, B2, respectively, in Fig. 9a). A marked decrease in thickness from 0.5 s TWT in the hanging wall of the Breiflabb Fault to 0.1 s TWT in its footwall suggests that the Breiflabb Fault was active early during rifting and that sub- and supra-salt deformation was coupled (Figs 8a and 9a). Depocentre B2 is thickest (up to 1.2 s TWT) in the immediate hanging wall of the Steinbit South Fault and is notably thinner in

Basin Research published by International Association of Sedimentologists and European Association of Geoscientists and Engineers and John Wiley & Sons Ltd.

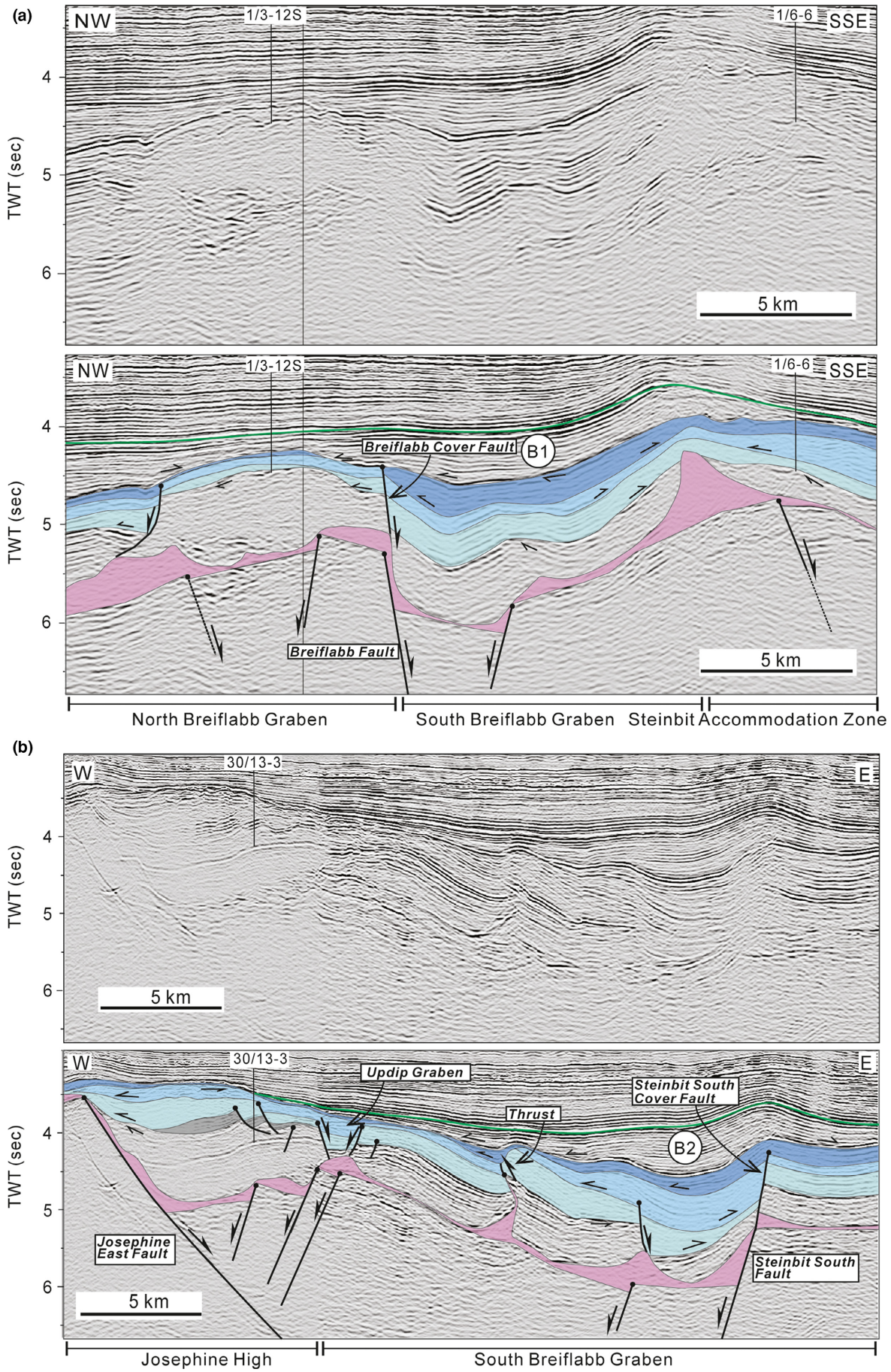

Basin Research published by International Association of Sedimentologists and European Association of Geoscientists and Engineers and John Wiley & Sons Ltd.

Fig. 8. Seismic sections (above) and their interpretations (below) illustrating the structural style and syn-rift depocentre geometry in the northern segment of the Central Graben. (a) NW–SSE section across the Brieflabb grabens. Note Breiflabb Fault dissecting the North and South Breiflabb Grabens. (b) E–W section across the South Breiflabb Graben and Josephine High. Note the thin-skinned deformation occur within the pre-rift on the hangingwall dipslope to the Steinbit South Fault. B1 and B2 relate to description in the text. See Fig. 5 for legend; Fig. 1b for location. Seismic data courtesy of CGG.

its footwall (*ca*. 500 ms TWT) (Fig. 8b). However, SU1 thins towards the fault, whereas SU2 thickens into the immediate hanging wall and is markedly thinner in the footwall (Figs 8b and 10). Thus, in a similar way to the Gert Fault, the Steinbit South Fault is interpreted to have propagated upward from sub-salt levels, initially folding the top pre-rift depositional surface and then breaching it to create a through-going, surface-breaking fault (Fig. 8b).

A series of small sub-basins with thickened SU2 and SU3 occur on the easterly tilted hanging wall dipslope to the Steinbit South Fault, updip of depocentre B2 (Fig. 8b). SU2 and SU3 are thickest (up to 0.4 s TWT) in a graben at the crest of the dipslope, and in a prominent thrust-bounded growth syncline (up to 0.5 s TWT thick) approximately 5 km to the east down the hanging wall dipslope (Fig. 8b). Both the updip graben and the thrust-related growth syncline are located above pre-rift diapirs,

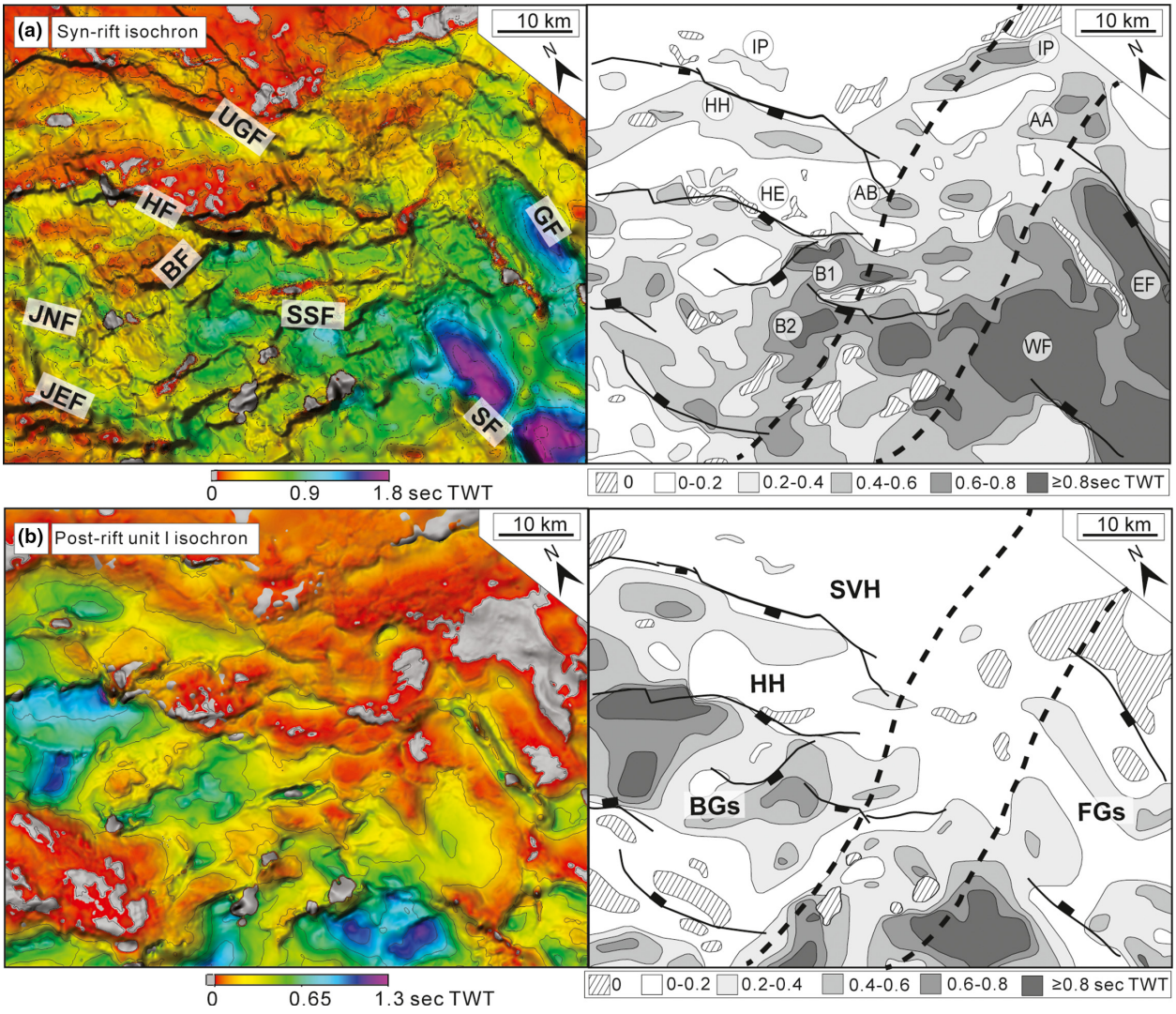

Fig. 9. Isochron maps of syn-rift and post-rift unit I seismic units. (a) Syn-rift isochron map overlain two-way travel-time (TWT) structure map of the base salt horizon (left) and simplified interpretation (right). (b) Post-rift unit I isochron map overlain TWT structure map of base post-rift horizon (left) and simplified interpretation (right). Fault abbreviations: UGF, Ula-Gyda Fault; HF, Hidra Fault; BF, Breiflabb Fault; JNF, Josephine North Fault; JEF, Josephine East Faut; SSF, Steinbit South Fault; GF, Gert Fault; SF, Skrubbe Fault. Area abbreviations: SVH, Sørvestlandet High; HH, Hidra High; BGs, Breiflabb grabens; FDs, Feda grabens. The two diagonal dashed lines delineate the Steinbit Accommodation Zone. Abbreviations in circles refer to description in the main text.

Basin Research published by International Association of Sedimentologists and European Association of Geoscientists and Engineers and John Wiley & Sons Ltd.

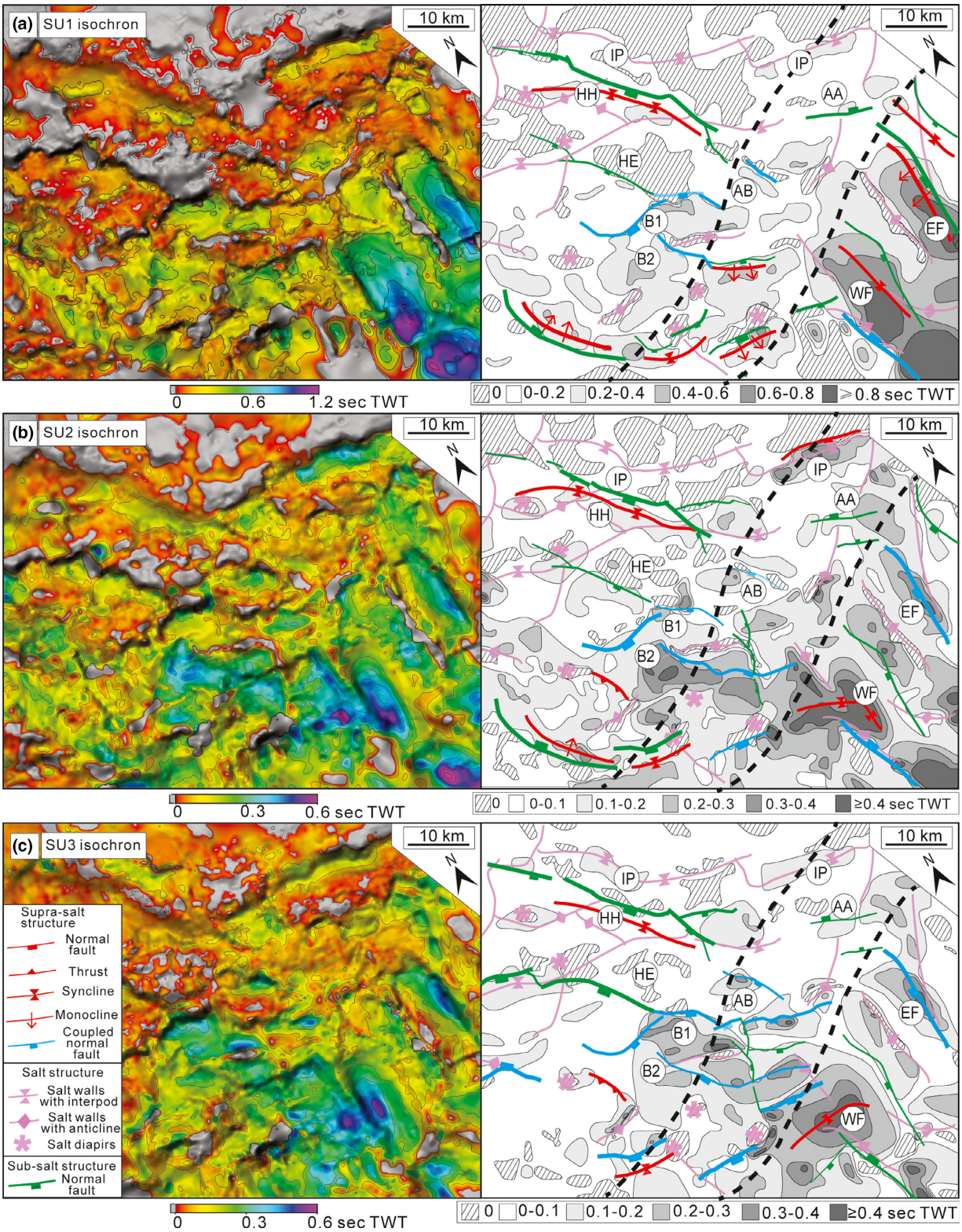

Fig. 10. Syn-rift isochron maps of seismic units SU1–3 (left) and interpreted structure activity maps for the main sub-salt, salt and supra-salt structures (right). (a) SU1 isochron map overlain two-way travel-time (TWT) structure map of base syn-rift horizon (left) and simplified interpretation (right). (b) SU2 isochron map overlain TWT structure map of base syn-rift horizon (left) and simplified interpretation (right). (c) SU3 isochron map overlain TWT structure map of base syn-rift horizon (left) and simplified interpretation (right). The two diagonal dashed lines delineate the Steinbit Accommodation Zone. Abbreviations in circles refer to description in the main text.

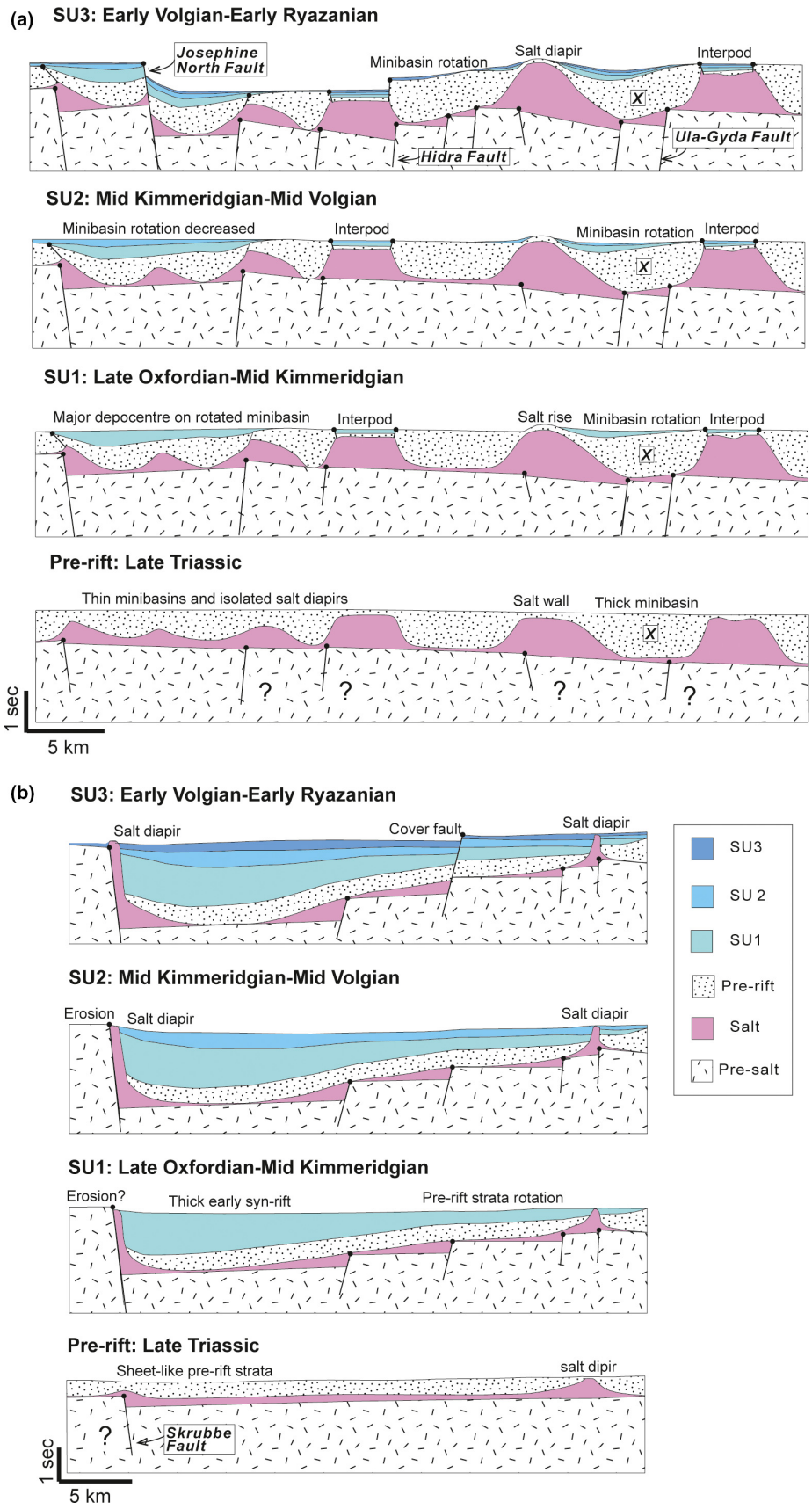

Fig. 11. Tectono-stratigraphic evolution of the Late Jurassic syn-rift in the Norwegian Central Graben. (a) Schematic tectono-stratigraphic evolution of the area where the minibasins and salt walls/diapirs dominate the pre-rift salt-related structures. Note the early syn-rift depocentres are over the rotated minibasins and interpods. (b) Schematic tectono-stratigraphic evolution of the East Feda Graben where the sheet-like pre-rift strata dominate. See the text for discussion.

Basin Research published by International Association of Sedimentologists and European Association of Geoscientists and Engineers and John Wiley & Sons Ltd.

and the adjacent pre-rift minibasins show little internal deformation (Fig. 8b). This range of structures is interpreted to have resulted from tilting of the hanging wall dipslope into Steinbit South Fault and sliding of the minibasins on the salt (Fig. 8b).

Another variation in syn-rift depocentre geometry and evolution is seen in the syn-rift depocentre on the Hidra High to the northeast of the Breiflabb grabens. Here, the syn-rift depocentre has a major synclinal form and is located along the SW margin of a thick, pre-rift minibasin (X in Fig. 5), and some 5 km into the hanging wall of the Ula-Gyda Fault (HH in Fig. 9a; Fig. 5). This depocentre is 50 km long and 8 km wide, with up to 0.6 s TWT of syn-rift strata (Fig. 5a, b). The individual syn-rift units have a symmetrical, synclinal form. SU1 and SU2 are relatively thick, each with an average thickness of 0.2 s TWT, whereas SU3 is <0.05 s TWT thick (Fig. 10). The location and form of this syn-rift depocentre, although controlled in part by the growth of the Ula-Gyda Fault, is also influenced by interaction between the fault and the thick pre-rift minibasin. In this case, the sub-salt Ula-Gyda Fault could not propagate through the thick minibasin, and instead causes the minibasin to tilt southwestward, away from the fault (Fig. 5). The tilting is interpreted to have been facilitated by salt flow into the hanging wall of Ula-Gyda Fault and into the salt wall to the southwest (Fig. 5).

Steinbit Accommodation Zone

The syn-rift structural style varies across the Steinbit Accommodation Zone at both sub-salt and supra-salt levels (Fig. 6). In the eastern, rift margin, part of the accommodation zone, syn-rift depocentres are asymmetrical interpods, for example, above salt wall W (Fig. 6c). They typically lie above salt walls and are largely decoupled from sub-salt normal faults. Further west, towards the rift axis, the syn-rift succession is relatively uniform in thickness, between 0.3–0.4 s TWT, with only small, local depocentres developed (e.g. AA in Figs 6c and 10), despite a complex sub-salt fault network (Figs 1b and 3a). These syn-rift depocentres tend to be located in the hanging wall of supra-salt faults that dissect thick pre-rift minibasins, but are decoupled from the sub-salt normal fault network (e.g. Fig. 6c).

To the west, where the Steinbit Accommodation Zone crosses the axis of the Norwegian Central Graben, syn-rift depocentres are typically <10 km long and <5 km wide, with up to 0.8 s TWT of syn-rift stratigraphy (e.g. AB in Figs 6b and 9a). The thickest syn-rift is generally located in the hanging wall of the larger sub-salt normal faults affecting the accommodation zone; these faults are typically fully coupled, through-going faults that affect sub-salt and cut through the thin to thick (0.3–0.8 s TWT) pre- and syn-rift strata (Fig. 6b).

DISCUSSION

This regional study of the Norwegian Central Graben has used merged, regionally extensive 3D seismic data to investigate first-order controls on structural style and tectono-sedimentary development in a salt-influenced rift with spatially different pre-rift salt-related structures and a variety of sub-salt normal faults. Based on analysis of the syn-rift depocentres and sub- and supra-Zechstein Supergroup structure, two factors stand out as major controls on the variability of syn-rift depocentres: (i) the throw and spacing of the rift-related sub-salt fault network, and (ii) the distribution of mobile salt and the associated variability in pre-rift salt tectonics. These factors are interpreted to have interacted to create the variability in the Late Jurassic syn-rift structural style in the Norwegian Central Graben. In the following section we discuss the variation over several tens of kilometres between different structural domains within the rift that introduces a large-scale organisation to the structural style and distribution of syn-rift depocentres (Fig. 12), and recognise six main structural styles within salt-influenced rifts (Fig. 13).

Sub-salt fault control on syn-rift structural style and depocentres

Studies of salt-free rifts, such as the East African Rift and the Suez Rift, have highlighted along-strike segmentation of rifts into rift segments separated by rift-wide accommodation zones (e.g. Rosendahl, 1987; Gawthorpe & Hurst, 1993; Moustafa, 1996; Younes & McClay, 2002; Tesfaye *et al.*, 2008; Fossen *et al.*, 2010). Rift segments are characterised by a series of major tilted fault blocks, typically several tens of kilometres long and 10–15 km wide, that are bounded by crustal-scale, hard-linked normal faults with several kilometres of displacement. In contrast to the major tilted fault blocks within rift axis segments, rift accommodation zones typically form broad zones of relative high topography that cross the rift axis and are associated with high fault density and low fault displacement (e.g. Rosendahl, 1987; Gawthorpe & Hurst, 1993; Morley, 1995; Faulds & Varga, 1998; McClay *et al.*, 2002; Younes & McClay, 2002). Previous studies of salt-influenced rifts have tended to focus on the detailed analysis of individual sub-salt fault systems (e.g. Stewart *et al.*, 1996; Richardson *et al.*, 2005; Duffy *et al.*, 2013; Jackson & Lewis, 2015) and have not considered the large-scale structural organisation of the rift segments and rift accommodation zones. Despite the potential for the salt to decouple sub-salt deformation from supra-salt deformation as cited in several papers (e.g. Stewart *et al.*, 1996), there is a recognisable relationship between the large-scale, sub-salt rift structure and the Late Jurassic syn-rift depocentres.

Our studies of the Norwegian Central Graben show large-scale rift segmentation into a northern rift segment, comprising the Hidra High and the North and South

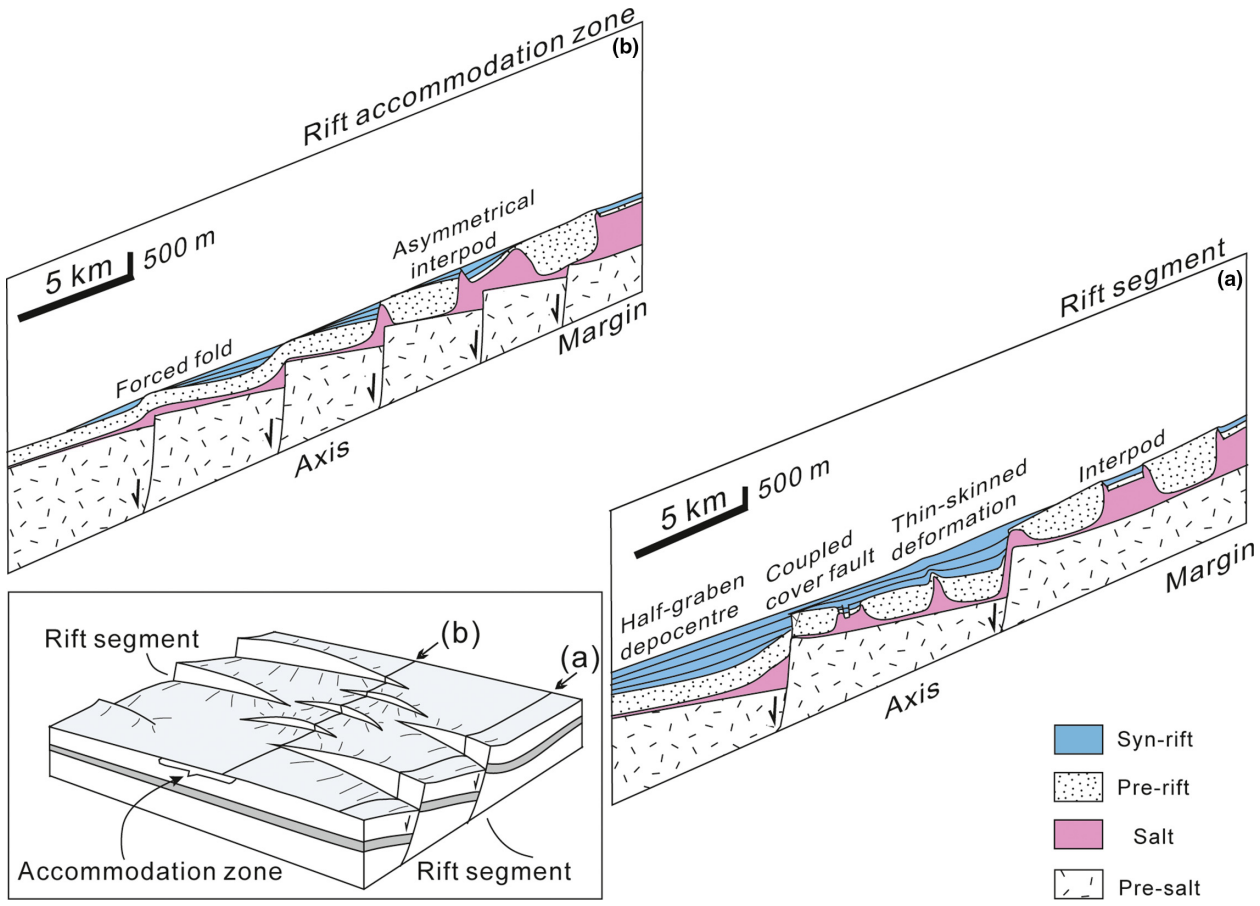

Fig. 12. Schematic sections illustrating the style and distribution of syn-rift depocentres in a typical salt-influenced rift comprising rift segments and rift accommodation zones. Inset shows the contrasting sub-salt normal fault and basin geometry of rift segments and rift accommodation zone.

Breiflabb grabens, and a southern segment comprising the East and West Feda grabens. The rift segments are separated from each other by the Steinbit Accommodation Zone. At the base salt horizon, the Steinbit Accommodation Zone shows many features typical of rift accommodation zones. For example, it is shallower (4.5–5.5 s TWT deep) than adjacent rift segments (>6 s TWT deep), and has higher fault density, with smaller fault spacing (typically to 2–5 km) (Fig. 3a). The Late Jurassic syn-rift depocentres in the accommodation zone are also relatively small, usually 5–10 km long, <5 km wide and are typically <1 s TWT thick (Figs 9a and 12). In contrast, the syn-rift depocentres in the rift segments are much larger, typically several tens of kilometres long, parallel to the strike of sub-salt faults, more than 10 km wide, and contain up to 1.8 s TWT of syn-rift stratigraphy (e.g. the Feda grabens) (Figs 9a and 12).

Within salt-free rifts there is also a distinction between the rift margin fault blocks and those along the rift axis in terms of their displacement and longevity, as strain localisation towards the rift axis tends to promote high displacement and longer activity along the axis of the rift (e.g. Gawthorpe *et al.*, 2003; Cowie *et al.*, 2005). Along the eastern rift margin of both the rift segments and the Steinbit Accommodation Zone, the sub-salt faults have much smaller throws, typically <100–200 ms TWT, than those towards the rift axis (Fig. 1b). Consequently, the syn-rift depocentres along the rift margin are largely unrelated to sub-salt normal faulting. They mainly occur as interpods above pre-rift salt walls and diapirs and are decoupled from and often strike obliquely to the sub-salt normal faults (Figs 5 and 12).

Detailed comparison of the syn-rift isochron map and the base salt TWT structure map (Figs 1b and 9a), suggests that the decoupling effect of salt does influence syn-rift structural style and basin evolution. The syn-rift depocentres in the rift axis are generally wider than the average sub-salt fault spacing in both the rift segments and the Steinbit Accommodation Zone (Figs 1b, 3a and 9). This is because small-throw sub-salt faults tend to be fully decoupled from supra-salt deformation by the salt (Koyi *et al.*, 1993; Stewart *et al.*, 1996; Withjack & Callaway, 2000). In the Norwegian Central Graben, sub-salt faults with throws <300 ms TWT are typically decoupled from deformation above the salt. Therefore, despite the high density of sub-salt faults (Fig. 3a), only large-throw faults in the rift axis are able to fully couple with supra-salt deformation and directly control syn-rift

Basin Research published by International Association of Sedimentologists and European Association of Geoscientists and Engineers and John Wiley & Sons Ltd.

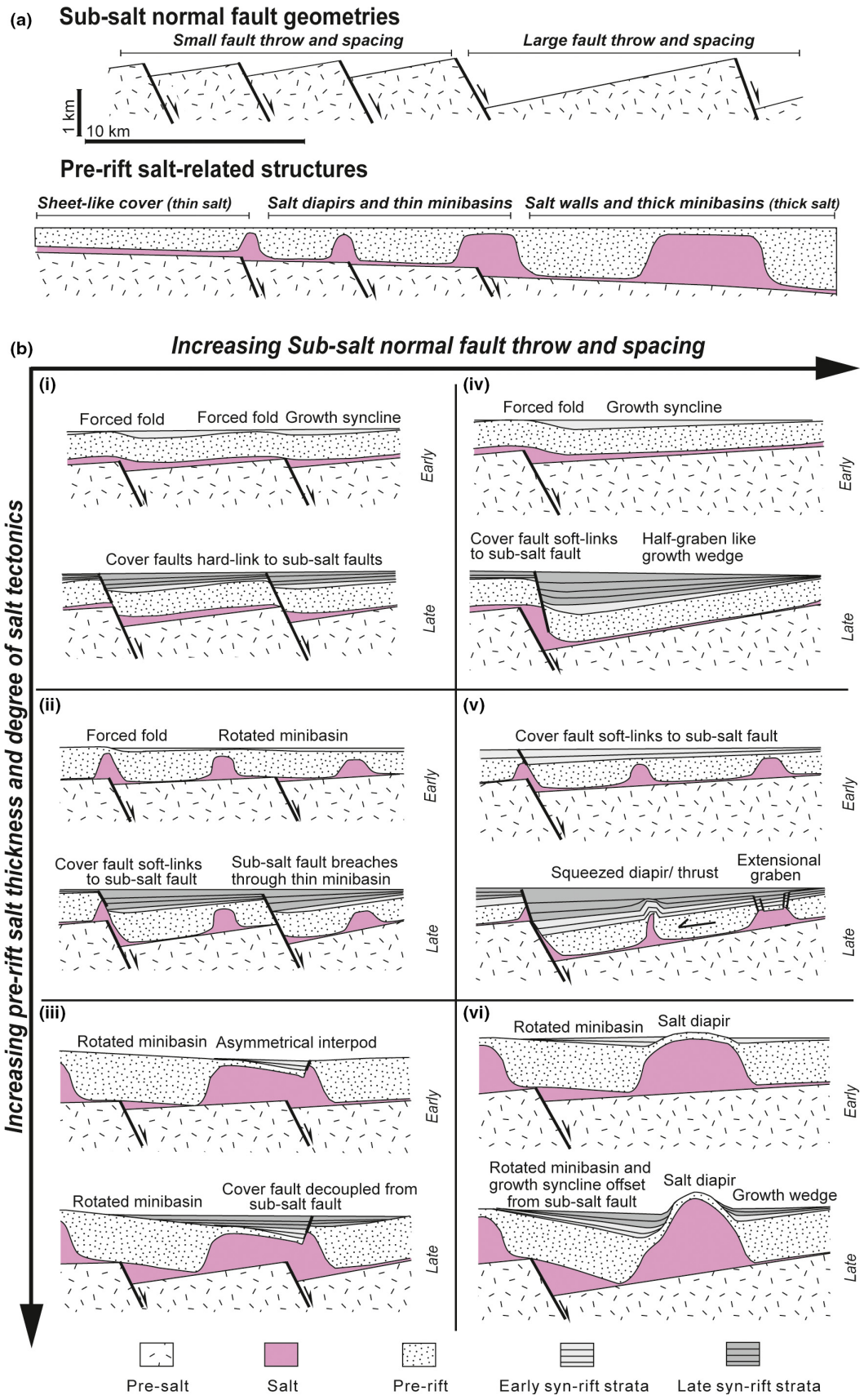

Fig. 13. Summary of the impact of varying sub-salt normal faulting and pre-rift salt-related structures on the structural style and evolution in salt-influenced rifts. (a) Summary of the main variations in sub-salt fault geometries and pre-rift salt-related structure styles observed in the study area. (b) Matrix of the six syn-rift depocentre geometries that result from the interaction between sub-salt normal faulting and pre-rift salt tectonics. See the text for discussion.

Basin Research published by International Association of Sedimentologists and European Association of Geoscientists and Engineers and John Wiley & Sons Ltd.

depocentre evolution (cf. Jackson & Rotevatn, 2013) (Fig. 10). In the rift segments, these large-throw faults are essentially basin-bounding faults that are tens of kilometres long, with >10 km fault spacing and typically 1000–2000-ms TWT throws (e.g. Ula-Gyda Fault, Fig. 5; Skrubbe Fault, Fig. 7b). In Steinbit Accommodation Zone, the larger sub-salt normal faults are much smaller, with 5–10 km fault spacing and <900 ms TWT throws (Fig. 6b).

Thus, in the Norwegian Central Graben, the underlying rift segmentation exerts an influence on the syn-rift depocentre development (Fig. 12), despite varying degrees of coupling between sub-salt and supra-salt deformation (Fig. 13). The variable impact of the salt and pre-rift salt-tectonic structures on the syn-rift depocentre geometry is discussed in the following section.

Pre-rift salt tectonic structural style control on syn-rift structural style and depocentres

Three different pre-rift salt tectonic styles have been recognised in the Norwegian Central Graben: (i) sheet-like pre-rift strata with thin salt and limited salt tectonics, (ii) isolated salt diapirs and thin minibasins, and (iii) elongate, connected salt walls and thick minibasins (Figs 5a and 7b). The formation of these different salt-related structures, prior to Late Jurassic rifting, relates to the original salt thickness and its mobility. Thicker salt accumulations allow the formation of larger minibasins and salt walls, whereas thinner salt favours the development of more sheet-like pre-rift strata that lack significant salt tectonics (e.g. Smith *et al.*, 1993) (Fig. 13a). In turn, the original salt thickness is controlled by the basin physiography at the time of salt deposition (Smith *et al.*, 1993; Clark *et al.*, 1998).

Previous studies of the influence of salt within pre-rift stratigraphy on syn-rift structural style and evolution have largely focused on the role of the autochthonous salt unit in decoupling sub-salt normal faulting from supra-salt deformation (e.g. Stewart *et al.*, 1996; Withjack & Callaway, 2000; Richardson *et al.*, 2005; Marsh *et al.*, 2010; Duffy *et al.*, 2013). In contrast, the role of mechanical heterogeneity within the pre-rift, related to relatively weak salt-cored structures, such as diapirs and salt walls compared to relatively strong minibasin fill has been largely overlooked. For the simplest pre-rift salt tectonic structural style observed in the Norwegian Central Graben, sheet-like pre-rift with limited salt tectonics, the pre-rift generally deforms by forced folding or faulting above sub-salt faults. Syn-rift depocentres in these situations are characterised by growth synclines and half-graben geometries (Fig. 13bI, bII, bIV). Similar syn-rift structural styles and basin geometries have been documented extensively in other salt-influenced rift basins, such as Rhine Graben, UK Central Graben, Danish Central Graben and South Viking Graben (e.g. Stewart *et al.*, 1996, 1997; Maurin & Niviere, 2000; Kane *et al.*, 2010; Duffy *et al.*, 2013).

The mechanical strength contrast between the pre-rift and salt is more prominent where pre-rift salt tectonics is characterised by small minibasins and isolated diapirs, which covers a large part of the Breiflabb Graben and the southern part of the Steinbit Accommodation Zone (Figs 6b and 8b). The relatively weak salt diapirs localise strain and deformation, whereas the minibasins behave as individual strong units within the pre-rift (Fig. 13bV). One example of this is on the hanging wall dipslope of the Steinbit South Fault in the South Breiflabb Graben. Here, tilting of the hanging wall dipslope triggered gravitational thin-skinned deformation, with normal faults and thrusts occurring locally above pre-rift salt diapirs while the pre-rift minibasin stratigraphy is largely undeformed and simply slide down the dipslope on the salt (Fig. 8b). Similar thin-skinned deformation has also been observed in United Kingdom West Central Graben (e.g. Stewart & Clark, 1999).

The localisation of syn-rift strain by salt-cored structures becomes more pronounced where minibasins are thick and bounded by elongate salt walls, for example, along the Ula-Gyda Fault (Fig. 5a, b). In this situation, sub-salt normal faults fail to propagate through the strong minibasins; rather, the minibasins rotate above the upward-propagating sub-salt fault, and pre-rift strata deformation is accommodated by the salt (Fig. 11a). As a result, syn-rift synclinal depocentres are located above the down-tilted edge of the thick minibasins and are offset a few kilometres into the hanging wall of sub-salt normal fault (Figs 11a and 13bVI). In contrast, where sub-salt normal faults occur beneath salt walls or thin minibasins, as the pre-rift strata are relatively thin, the pre-rift strata may be breached forming a depocentre in the immediate hanging wall (Figs 6c and 13bIII).

In the absence of major normal faulting, such as along the rift margin, the local subsidence mechanism for syn-rift basin development is largely controlled by local salt tectonics that continues from earlier pre-rift times (Fig. 12). This tectono-stratigraphic response during syn-rift times is best illustrated along the Sørvestlandet High, where Late Jurassic depocentres occur as interpods located above elongate salt walls (e.g. Fig. 5a, b). The mechanisms of interpod development have been discussed by several workers and includes regional extension or salt dissolution (Hodgson *et al.*, 1992; Smith *et al.*, 1993; Clark *et al.*, 1999; Kane *et al.*, 2010; Mannie *et al.*, 2014). One of the key characteristics of interpods is that they are not strongly linked to sub-salt normal faults (e.g. Fig. 5a).

CONCLUSIONS

Regionaly consistent interpretation of well-calibrated 3D seismic data from the Norwegian Central Graben permits tectono-stratigraphic analysis of the Late Jurassic–Early Cretaceous rifting and assessment of rifting and salt tectonics on the structural style and evolution of salt-influenced rifts. The fault network within the pre-Zechstein

Basin Research published by International Association of Sedimentologists and European Association of Geoscientists and Engineers and John Wiley & Sons Ltd.

interval can be divided into northern and southern rift segments characterised by rift margin and rift axis domains, separated by a rift-wide accommodation zone, here called the Steinbit Accommodation Zone. Within the rift segments, sub-salt normal faults are larger, in terms of fault throw, length and spacing, compared to the accommodation zone, which has a higher density of smaller normal faults.

Isochron maps show that Zechstein salt and pre-rift strata range from sheet-like strata with thin salt and minor salt tectonics, to elongate, connected salt walls and thick minibasins. This variability reflects the original salt thickness and degree of salt tectonics prior to rifting. The salt and salt-related structures played an important role in creating mechanical heterogeneity within the pre-rift strata that, during rifting, influenced the growth of the post-salt, rift-related normal fault network. Pre-rift minibasins and sheet-like pre-rift strata formed relatively strong units within the pre-rift stratigraphy, whereas the pre-rift salt walls and diapirs were weak and tended to localise strain and accommodate deformation.

Our analysis of the Norwegian Central Graben has allowed us to identify six styles of interaction between the sub-salt normal faults and pre-rift salt-related structures. At the rift scale, the syn-rift structural style and tectono-stratigraphic evolution are strongly influenced by the segmentations of the rift. Salt thickness and the style of pre-rift salt tectonics modify the post-salt structural style. The pre-rift salt distribution and salt tectonics are, in turn strongly influenced by the basin configuration at the time of deposition of the salt, which may be significantly different to that during the later rift phase.

In rift margin locations, characterised by low displacement normal faults, syn-rift deposition may be mainly controlled by pre-rift salt tectonics and unrelated to the local sub-salt normal fault network. In contrast, rift axis settings are dominated by sub-salt normal faults, causing forced folding or faulting of the post-salt section and creating relatively simply half graben depocentres. Nevertheless, fault block tilting may stimulate down-dip flow of the salt and the development of thin-skinned deformation above the salt horizon, creating additional local depocentres. The failure of sub-salt normal faults to propagate through mechanically strong, thick minibasins creates synclinal growth wedges located away from the faults, largely driven by rotation of the thick minibasins and flow of the salt.

This study suggests that current structural and tectono-stratigraphic models of salt-influenced rifts need to be revised to take into account the complex interaction between normal faulting and heterogeneity of the pre-rift caused by pre-rift salt tectonics. Furthermore, the variations in structural style and tectono-stratigraphic evolution within salt-influenced rift presented in this paper also provides a framework to assess sedimentary response and facies distributions within salt-influenced rift basins.

ACKNOWLEDGEMENTS

The project was supported by Total E&P Norge. We acknowledge CGG and PGS for providing access to seismic data and giving permission to publish the seismic sections in this paper. Jonathan Wonham provided advice during the early stage of the study and Rob Lidster and Tore Lein Mathisen are thanked for constructive discussions on seismic interpretation. Schlumberger is thanked for providing Petrel software in the 3D Seismic Lab in the University of Bergen. Constructive reviews from Bruce Trudgill and Matt Lewis, and editorial comments from Rebecca Bell, are thanked for improving the manuscript. The conclusions drawn within this publication are those of the authors and do not reflect the views of Total E&P Norge or their partners within the study area.

REFERENCES

Alves, T.M., Gawthorpe, R.L., Hunt, D.W. & Monteiro, J.H. (2002) Jurassic tectono-sedimentary evolution of the Northern Lusitanian Basin (offshore Portugal). *Mar. Pet. Geol.*, **19**, 727–754.

Callot, J.-P., Trocmé, V., Letouzey, J., Albouy, E., Jahani, S. & Sherkati, S. (2012) Pre-existing salt structures and the folding of the Zagros mountains. *Geol. Soc. London. Spec. Publ.*, **363**, 545–561.

Clark, J.A., Stewart, S.A. & Cartwright, J.A. (1998) Evolution of the NW margin of the North Permian Basin, UK North Sea. *J. Geol. Soc.*, **155**, 663–676.

Clark, J., Cartwright, J. & Stewart, S. (1999) Mesozoic dissolution tectonics on the West Central Shelf, UK Central North Sea. *Mar. Pet. Geol.*, **16**, 283–300.

Coward, M.P. (1995) Structural and tectonic setting of the Permo-Triassic basins of northwest Europe. *Geol. Soc. London. Spec. Publ.*, **91**, 7–39.

Cowie, P.A., Gupta, S. & Dawers, N.H. (2000) Implications of fault array evolution for synrift depocentre development: insights from a numerical fault growth model. *Basin Res.*, **12**, 241–261.

Cowie, P.A., Underhill, J.R., Behn, M.D., Lin, J. & Gill, C.E. (2005) Spatio-temporal evolution of strain accumulation derived from multi-scale observations of Late Jurassic rifting in the northern North Sea: a critical test of models for lithospheric extension. *Earth Planet. Sci. Lett.*, **234**, 401–419.

Dooley, T., McClay, K.R. & Pascoe, R. (2003) 3D analogue models of variable displacement extensional faults: applications to the Revfallet Fault system, offshore mid-Norway. *Geol. Soc. London. Spec. Publ.*, **212**, 151–167.

Duffy, O.B., Gawthorpe, R.L., Docherty, M. & Brocklehurst, S.H. (2013) Mobile evaporite controls on the structural style and evolution of rift basins: Danish Central Graben, North Sea. *Basin Res.*, **25**, 310–330.

Erratt, D., Thomas, G.M. & Wall, G.R.T. (1999) The evolution of the Central North Sea Rift. In: *Petroleum Geology of Northwest Europe: Proceedings of the 5th Conference* (Ed. by A.J. Fleet, S.A.R. Boldy), pp. 63–82. The Geological Society, London.

Faulds, J.E. & Varga, R.J. (1998) The role of accommodation zones and transfer zones in the regional segmentation

of extended terranes. *Geol. Soc. Am. Spec. Pap.*, **323**, 1–45.

Fossen, H., Schultz, R.A., Rundhovde, E., Rotevatn, A. & Buckley, S.J. (2010) Fault linkage and graben stepovers in the Canyonlands (Utah) and the North Sea Viking Graben, with implications for hydrocarbon migration and accumulation. *AAPG Bull.*, **94**, 597–613.

Fraser, S.I., Robinson, A.M., Johnson, H.D., Underhill, J.R., Kadolsky, D.G.A., Conell, R., Johannesen, P. & Ravnås, R. (2003) Upper Jurassic. In: *The Millenium Atlas: Petroleum Geology of the Central and Northern North Sea* (Ed. by D. Evans, C. Graham, A. Armour & P. Bathurst), pp. 157–189. The Geological Society, London.

Gawthorpe, R.L. & Hurst, J.M. (1993) Transfer zones in extensional basins: their structural style and influence on drainage development and stratigraphy. *J. Geol. Soc.*, **150**, 1137–1152.

Gawthorpe, R.L. & Leeder, M.R. (2000) Tectono-sedimentary evolution of active extensional basins. *Basin Res.*, **12**, 195–218.

Gawthorpe, R.L., Sharp, I., Underhill, J.R. & Gupta, S. (1997) Linked sequence stratigraphic and structural evolution of propagating normal faults. *Geology*, **25**, 795–798.

Gawthorpe, R.L., Jackson, C.A.L., Young, M.J., Sharp, I.R., Moustafa, A.R. & Leppard, C.W. (2003) Normal fault growth, displacement localisation and the evolution of normal fault populations: the Hammam Faraun fault block, Suez rift, Egypt. *J. Struct. Geol.*, **25**, 883–895.

Gowers, M.B. & Sæbøe, A. (1985) On the structural evolution of the Central Trough in the Norwegian and Danish sectors of the North Sea. *Mar. Pet. Geol.*, **2**, 298–318.

Gowers, M.B., Holtar, E. & Swensson, E. (1993) The structure of the Norwegian Central Trough (Central Graben area). In: *Petroleum Geology of Northwest Europe: Proceedings of the 4th Conference* (Ed. by J.R. Parker), pp. 1245–1254. The Geological Society, London.

Gradstein, F.M., Anthonissen, E., Brunstad, H., Charnock, M., Hammer, O., Hellem, T. & Lervik, K.S. (2010) Norwegian Offshore Stratigraphic Lexicon (Norlex). *Newsl. Stratigr.*, **44**, 73–86.

Gupta, S., Cowie, P.A., Dawers, N.H. & Underhill, J.R. (1998) A mechanism to explain rift-basin subsidence and stratigraphic patterns through fault-array evolution. *Geology*, **26**, 595–598.

Hodgson, N.A., Farnsworth, J. & Fraser, A.J. (1992) Salt-related tectonics, sedimentation and hydrocarbon plays in the Central Graben, North Sea, UKCS. *Geol. Soc. London. Spec. Publ.*, **67**, 31–63.

Hudec, M.R. & Jackson, M.P. (2007) Terra infirma: understanding salt tectonics. *Earth-Sci. Rev.*, **82**(1), 1–28.

Husmo, T., Hamar, G., Høiland, O., Johannessen, E., Rømuld, A., Spencer, A. & Titterton, R. (2002) Lower and Middle Jurassic. In: *The Millennium Atlas: Petroleum Geology of the Central and Northern North Sea* (Ed. by D. Evans, C. Graham, A. Armour, P. Bathurst), pp. 129–155. The Geological Society, London.

Jackson, C.A.L. & Lewis, M.M. (2015) Structural style and evolution of a salt-influenced rift basin margin; the impact of variations in salt composition and the role of polyphase extension. *Basin Res.*, **28**, 81–102.

Jackson, C.A.L. & Rotevatn, A. (2013) 3D seismic analysis of the structure and evolution of a salt-influenced normal fault zone: a test of competing fault growth models. *J. Struct. Geol.*, **54**, 215–234.

Kane, K.E., Jackson, C.A.-L. & Larsen, E. (2010) Normal fault growth and fault-related folding in a salt-influenced rift basin: South Viking Graben, offshore Norway. *J. Struct. Geol.*, **32**, 490–506.

Karlo, J.F., van Buchem, F.S., Moen, J. & Milroy, K. (2014) Triassic-age salt tectonics of the Central North Sea. *Interpretation*, **2**, 19–28.

Koyi, H., Jenyon, M.K. & Petersen, K. (1993) The effect of basement faulting on diapirsm. *J. Pet. Geol*, **16**, 285–312.

Letouzey, J., Colletta, B., Vially, R. & Chermette, J. (1995) Evolution of salt-related structures in compressional settings. In: *Salt Tectonics: A Global Perspective* (Ed. by M.P.A. Jackson, D.G. Roberts & S. Snelson) *AAPG Memoir.*, **65**, 41–69. AAGP.

Lewis, M.M., Jackson, C.A.L. & Gawthorpe, R.L. (2013) Salt-influenced normal fault growth and forced folding: the Stavanger Fault System, North Sea. *J. Struct. Geol.*, **54**, 156–173.

Mannie, A.S., Jackson, C.A.-L. & Hampson, G.J. (2014) Shallow-marine reservoir development in extensional diapir-collapse minibasins: an integrated subsurface case study from the Upper Jurassic of the Cod Terrace, Norwegian North Sea. *AAPG Bull.*, **98**, 2019–2055.

Marsh, N., Imber, J., Holdsworth, R.E., Brockbank, P. & Ringrose, P. (2010) The structural evolution of the Halten Terrace, offshore Mid-Norway: extensional fault growth and strain localisation in a multi-layer brittle–ductile system. *Basin Res.*, **22**, 195–214.

Maurin, J.-C. & Niviere, B. (2000) Extentional forced folding and decollement of the pre-rift series along the Rhine Graben and their influence on the geometry of the syn-rift sequences. *Geol. Soc. London. Spec. Publ.*, **169**, 73–86.

McClay, K.R., Dooley, T., Whitehouse, P. & Mills, M. (2002) 4-D evolution of rift systems: insights from scaled physical models. *AAPG Bull.*, **86**, 935–959.

Mohr, M., Kukla, P., Urai, J. & Bresser, G. (2005) Multiphase salt tectonic evolution in NW Germany: seismic interpretation and retro-deformation. *Int. J. Earth Sci.*, **94**, 917–940.

Morley, C.K. (1995) Developments in the structural geology of rifts over the last decade and their impact on hydrocarbon exploration. *Geol. Soc. London. Spec. Publ.*, **80**, 1–32.

Moustafa, A.R. (1996) Internal structure and deformation of an accommodation zone in the northern part of the Suez rift. *J. Struct. Geol.*, **18**, 93–107.

Rasmussen, E.S., Lomholt, S., Andersen, C. & Vejbæk, O.V. (1998) Aspects of the structural evolution of the Lusitanian Basin in Portugal and the shelf and slope area offshore Portugal. *Tectonophysics*, **300**, 199–225.

Rattey, R.P. & Hayward, A.B. (1993) Sequence stratigraphy of a failed rift system: the Middle Jurassic to Early Cretaceous basin evolution of the central and northern North Sea. In: *Petroleum Geology of Northwest Europe: Proceedings of the 4th Conference* (Ed. by J.R. Parker), pp. 215–249. The Geological Society, London.

Rawson, P.F. & Riley, L.A. (1982) Latest Jurassic-Early Cretaceous events and the "Late Cimmerian Unconformity" in North Sea Area. *AAPG Bull.*, **66**, 2628–2648.

Richardson, N.J., Underhill, J.R. & Lewis, G. (2005) The role of evaporite mobility in modifying subsidence patterns during

Basin Research published by International Association of Sedimentologists and European Association of Geoscientists and Engineers and John Wiley & Sons Ltd.

normal fault growth and linkage, Halten Terrace, Mid-Norway. *Basin Res.*, **17**, 203–223.

Rosendahl, B.R. (1987) Architecture of continental rifts with special reference to East Africa. *Annu. Rev. Earth Planet. Sci.*, **15**, 445–503.

Rowan, M.G. & Vendeville, B.C. (2006) Foldbelts with early salt withdrawal and diapirism: physical model and examples from the northern gulf of mexico and the flinders ranges, Australia. *Mar. Pet. Geol.*, **23**, 871–891.

Schlische, R.W. (1995) Geometry and origin of fault-related folds in extensional settings. *AAPG Bull.*, **79**, 1661–1678.

Smith, R., Hodgson, N. & Fulton, M. (1993) Salt Control on Triassic Reservoir Distribution, UKCS Central North Sea. In: *Petroleum Geology of Northwest Europe: Proceedings of the 4th Conference* (Ed. by J.R. Parker), pp. 547–557. The Geological Society, London.

Stewart, S.A. (2007) Salt Tectonics in the North Sea Basin: a structural style template for seismic interpreters. *Geol. Soc. London. Spec. Publ.*, **272**, 361–396.

Stewart, S.A. & Clark, J.A. (1999) Impact of salt on the structure of the Central North Sea hydrocarbon fairways. In: *Petroleum Geology of Northwest Europe: Proceedings of the 5th Conference* (Ed. by A.J. Fleet, S.A.R. Boldy), pp. 179–200. The Geological Society, London.

Stewart, S.A. & Coward, M.P. (1995) Synthesis of salt tectonics in the southern North Sea, UK. *Mar. Pet. Geol.*, **12**, 457–475.

Stewart, S.A., Harvey, M.J., Otto, S.C. & Weston, P.J. (1996) Influence of salt on fault geometry: examples from the UK salt basins. *Geol. Soc. London. Spec. Publ.*, **100**, 175–202.

Stewart, S.A., Ruffell, A.H. & Harvey, M.J. (1997) Relationship between basement-linked and gravity-driven fault systems in the UKCS salt basins. *Mar. Pet. Geol.*, **14**, 581–604.

Stewart, S.A., Fraser, S., Cartwright, J., Clark, J. & Johnson, H. (1999) Controls on Upper Jurassic sediment distribution in the Durward-Dauntless area, UK Blocks 21/11, 21/16. In: *Petroleum Geology of Northwest Europe: Proceedings of the 5th Conference* (Ed. by A.J. Fleet, S.A.R. Boldy), pp. 879–896. The Geological Society, London.

Tesfaye, S., Rowan, M.G., Mueller, K., Trudgill, B.D. & Harding, D.J. (2008) Relay and accommodation zones in the Dobe and Hanle grabens, central Afar, Ethiopia and Djibouti. *J. Geol. Soc.*, **165**, 535–547.

Tvedt, A., Rotevatn, A., Jackson, C.A.-L., Fossen, H. & Gawthorpe, R.L. (2013) Growth of normal faults in multilayer sequences: a 3D seismic case study from the Egersund Basin, Norwegian North Sea. *J. Struct. Geol.*, **55**, 1–20.

Underhill, J.R. & Partington, M.A. (1993) Jurassic thermal doming and deflation in the North Sea: implications of the sequence stratigraphic evidence. In: *Petroleum Geology of Northwest Europe: Proceedings of the 4th Conference* (Ed. by J.R. Parker), pp. 337–345. The Geological Society, London.

Withjack, M.O. & Callaway, S. (2000) Active normal faulting beneath a salt layer: an experimental study of deformation patterns in the cover sequence. *AAPG Bull.*, **84**, 627–651.

Withjack, M.O., Olson, J. & Peterson, E. (1990) Experimental models of extensional forced folds. *AAPG Bull.*, **74**, 1038–1054.

Wonham, J., Rodwell, I., Lein-Mathisen, T. & Thomas, M. (2014) Tectonic control on sedimentation, erosion and redeposition of Upper Jurassic sandstones, Central Graben, North Sea. In: *From Depositional Systems to Sedimentary Successions on the Norwegian Continental Margin* (Ed. by A.W. Martinius, R. Ravnås, J.A. Howell, R.J. Steel & J.P. Wonham) *Int. Assoc. Sedimentol. Spec. Publ.*, **46**, 473–512.

Younes, A.I. & McClay, K. (2002) Development of accommodation zones in the Gulf of Suez-Red Sea Rift, Egypt. *AAPG Bull.*, **86**, 1003–1026.

Ziegler, P.A. (1982) *Geological Atlas of Western and Central Europe*. Elsevier Scientific Publishing Co., Amsterdam.

Ziegler, P.A. (1990) Tectonic and palaeogeographic development of the North Sea Rift system. In: *Tectonic Evolution of the North Sea Rifts* (Ed. by D.J. Blundell & A.D. Gibbs), pp. 1–36. Clarendon Press, Oxford.

Manuscript received 5 February 2016; In revised form 16 August 2016; Manuscript accepted 18 August 2016.